ity (LOH) leads to the detection of mutants [6]. Human lymphoblastoid TK6 and WTK-1 cells are also heterozygous at the *Tk* locus and are also widely used in the *Tk* mutation assay [7–10].

TK6 and WTK-1 cells are both derived from WIL-2 cells [11], but TK6 cells have a wild type p53 tumor suppressor gene while WTK-1 cells have a mutant p53 gene [12].

p53 is involved in DNA repair, the G_1 check point, and the induction of apoptosis [13]. Wild type p53 leads cells with repairable DNA damage into cell cycle arrest, allowing repair of the damage, and cells with severe DNA damage to apoptosis, although mutated p53 does not. Earlier studies have shown that, compared with p53 mutant or null cells, p53 wild type cells undergo apoptosis earlier or at a higher frequency following severe cytotoxicity induced by X-rays or certain chemicals [10,12,14–17]. p53 mutant cells differ from the wild type in their cytotoxic and mutagenic responses to some mutagens [3,18–20]. Some clastogens and spindle poisons are more cytotoxic in wild type cells than in mutant cells, and at equal levels of cytotoxicity, are more clastogenic in the mutant cells [10,21].

The spontaneous MF in WTK-1 cells is 100–200 $\times 10^{-6}$ while it is less than 10×10^{-6} in TK6 cells [3]. Furthermore WTK-1 cells are more resistant than TK6 cells to X-rays and other mutagens [3]. These differences may be due to differences in p53 status. Because TK6 and WTK-1 cells are genetically similar except for p53 status, they are useful for examining the function of p53 status.

p53 is mutated at codon 170 of exon 5 in MOLY cells and at codon 237 of exon 7 in WTK-1 cells [22]. Because both those codons are the part of the central DNA binding domain [13], it is likely that the mutant p53 proteins in MOLY and WTK-1 cells lose the same function. The spontaneous MF is about the same in MOLY [5] and WTK-1 cells, and MOLY cells are also more resistant to X-rays than p53 wild type cells [21]. Because no cell line with a wild type p53 gene has the same genomic background as MOLY cells, MOLY cells cannot be compared directly with a p53 wild type cell line. However the response of MOLY cells to mutagens is probably similar to that of WTK-1 cells, so MOLY cells would show the same genomic instability as WTK-1 cells (or other p53-mutated cells).

5-Fluorouracil (5-FU), a pyrimidine based analog, is used as an anticancer drug. When 5-FU is converted to 5-fluoro-2-deoxyuridylate monophosphate (FdUMP), it competitively inhibits DNA synthesis via inhibition of thymidylate synthetase (TS) [23–25]. 5-FU is metabolized by orotate phosphoribosyl transferase (OPRT) and thymidine phosphorylase (TP) and detoxified by dihydrouracil dehydrogenase (DPD) [24–27].

5-FU is clastogenic in mammalian cells [28] in vitro and in vivo [29], and is mutagenic to MOLY cells [5,30], but not to *Salmonella typhimurium* [28]. While 5-FU induces neither chromosomal aberrations nor sister chromatid exchanges in the human subjects studied so far [31], it is difficult to assess whether 5-FU is truly non-mutagenic in humans because all the human subjects have been patients. Furthermore, there are few reports on the mutagenicity or clastogenicity of 5-FU in human cell lines. Here we evaluated the mutagenicity and clastogenicity of 5-FU in human cell lines in an attempt to assess its risk to humans.

Because both WTK-1 and MOLY cells are p53 mutants, we were interested in determining whether both lines would respond similarly to 5-FU. We used both lines, and TK6 cells as well, to test the effects of 5-FU in the *Tk* and in vitro MN assays, and we also analyzed the effect of 5-FU on apoptosis and the cell cycle in each cell line. Furthermore we measured the activity of the 5-FU metabolizing enzymes (TS, DPD, OPRT, and TP) in each cell line.

2. Materials and methods

2.1. Chemicals

5-FU (CAS No. 51-21-8) was purchased from Wako Pure Chemicals Industries Ltd. (Osaka, Japan), and methyl methanesulfonate (MMS, CAS No. 66-27-3) from Aldrich Chemical Co. Inc. (Milwaukee, WI). 5-FU and MMS were dissolved in physiologic saline just before use. [6-^{14}C]–5-FU (1.85 GBq/mmol) and [6-^{3}H]–FdUMP (625 GBq/mmol) were purchased from Moravek Biochemicals Inc. (Brea, CA).

2.2. Cell lines and culture

MOLY, TK6, and WTK-1 cells were provided by Hatano Research Institute at the Food and Drug Safety Center. The cells were cultured in RPMI 1640 medium (Gibco, Invitrogen Corp., Carlsbad, CA) containing 10% (v/v) horse serum (JRH Biosciences, Lenexa, KS); 20% (v/v) horse serum was used to measure the plating efficiency and mutation frequency of MOLY cells. The cells were incubated at 37 °C in an atmosphere of 5% CO_2 and high humidity.

2.3. Selection of concentration

Considering its cytotoxicity, we tested 5-FU at 1, 2, 4, and 8 μg/mL in MOLY cells; 1.56, 3.13, 6.25, 12.5, and 25 μg/mL in TK6 cells; and 3.13, 6.25, 12.5, 25, and 50 μg/mL in WTK-1 cells. MMS was used as the positive control at 10 μg/mL in MOLY cells and 5 μg/mL in human cells.

2.4. Chemical treatment

In this study, MOLY cells doubled in 10.3 h, TK6 cells in 16.9 h, and WTK-1 cells in 19.9 h. Based on that, we treated MOLY cells for 3 h and the human cell lines for 4 h. We treated 1×10^7 cells (at 5×10^5/mL), with shaking, at 37 °C, washed them, adjusted them to a density of 2×10^5 cells/mL, and incubated them.

2.5. Tk assay

The *Tk* assay was performed by the microwell method [3,5]. A portion of the cells were seeded onto 96-well plates to measure the plating efficiency (PE) after 5-FU treatment (PE0). The remaining MOLY cells were incubated for 48 h and the human cells for 72 h to permit phenotypic expression. They were seeded onto 96-well plates in the presence of trifluorothymidine (TFT, CAS No. 70-00-8, Sigma Chemical Co., St. Louis, MO) for assessment of mutation frequency (MF). Another portion of the cells were seeded onto 96-well plates in the absence of TFT for the measurement of plating efficiency after the expression period (PE2 for MOLY cells, PE3 for TK6 and WTK-1 cells).

After incubation, the number of wells containing colonies were counted, and PE, MF, and relative survival (RS) from PE0 were calculated as previously described [5]. We also calculated the 5-FU concentration that caused 50% growth inhibition (IC_{50}) in RS0.

2.6. In vitro MN assay

We collected 10^6 to 3×10^6 cells 48 h after 5-FU treatment, and prepared the MN assay specimens as previously described [32]. The specimens stained with acridine orange (Wako) were observed with the aid of a fluorescence microscope with a 470–490 nm excitation filter. One thousand cells from each treatment group were observed and the number with MN was counted. To be judged a MN, the structure had to have a diameter that was less than half the diameter of the main nucleus. Cells having an abnormal main nucleus were excluded from this analysis.

2.7. Analysis of apoptosis and the cell cycle

For analysis of apoptosis and cell cycle distribution, we sampled 2×10^6 cells at 0.5, 24, and 48 h (all cell lines) or at 72 h (TK6 and WTK-1 cells) after 5-FU treatment. Apoptosis was analyzed by flow cytometry and nuclear morphology. For flow cytometry, MEBSTAIN Apoptosis Kit® (Medical & Biological Laboratories Co. Ltd., Nagoya, Japan), which is based on the TUNEL method [33,34], was used. The number of TUNEL-positive cells per 10,000 cells was determined with a flow cytometer (FACScan, Becton-Dickinson, San Diego, CA) equipped with a 488 nm argon-ion laser at 15 mW with a 530/30 nm bandpass filter.

For nuclear morphology analysis, the cells were stained with Hoechst 33342 solution (Wako) and observed with the aid of a fluorescence microscope with a 330–385 nm excitation filter.

For analysis of cell cycle distribution, the cells were fixed with 70% (v/v) ethanol at −20 °C overnight, and stained with propidium iodide (Wako) for 30 min at room temperature. Ten thousand cells were analyzed on FACScan with a 585/42 nm bandpass filter. Mod Fit LT ver. 1.00 (Verity Software House Inc., Topsham, ME) was used for cell cycle analysis.

2.8. Measurement of enzyme activity

2.8.1. TS content

TS content was determined by quantifying [6-^{3}H]–FdUMP binding sites in the 105,000 g supernatant (cytosol) of cell homogenates based on the method described by Spears et al. [35], with minor modifications [36]. The samples were incubated with [6-^{3}H]–FdUMP in the presence of 5,10-methylene tetrahydrofolate for 20 min at 30 °C and radioactivity in the acid-insoluble fraction was measured with a liquid scintillation counter.

2.8.2. DPD, OPRT, and TP activity

DPD activity were measured as previously described, with minor modifications [35,37]. Briefly, cell line enzyme solutions were incubated with a reaction mixture containing 2 mM dithiothreitol, 5 mM $MgCl_2$, 0.02 mM [6-^{14}C]–5-FU (56 nCi), and 100 mM NADPH at 37 °C for 10 or 30 min. The DPD activity was calculated as the ratio of the radioactivity of the catabolism fraction (dihydrofluorouracil and fluoro-β-alanine) to total radioactivity ([6-^{14}C]–5-FU plus the catabolism fraction).

OPRT activity was determined according to the modified method of Peters et al. [38] using [6-^{14}C]–5-FU (56 nCi) as the substrate. Cell line enzyme solutions were incubated with a reaction mixture containing 50 mM Tris–HCl buffer (pH 8.0), 10 mM NaF, 5 mM $MgCl_2$, 4 mM PRPP, and 0.02 mM [6-^{14}C]–5-FU (56 nCi) at 37 °C for 10 or 30 min. OPRT activity was calculated as the ratio of the radioactivity of the metabolism fraction (5-fluoro-2-deoxyuridylate monophosphate) to the total radioactivity ([6-^{14}C]–5-FU plus the metabolism fraction).

TP activity was measured as previously described [39]. Briefly, the cell line enzyme solution was incubated with a reaction mixture containing 50 mM Tris–HCl buffer (pH 8.0), 10 mM NaF, 5 mM $MgCl_2$, 4 mM deoxyribose-1-phosphate, 10 mM ATP, and 0.02 mM [6-^{14}C]–5-FU (56 nCi) at 37 °C for 10 or 30 min. TP activity was calculated as the ratio of the radioactivity of the metabolism fraction (5-fluorodeoxyuridine) to total radioactivity ([6-^{14}C]–5-FU plus the metabolism fraction).

2.9. Statistical analysis

We judged the *Tk* mutation assay as positive when treatment at least doubled the MF relative to the solvent control and linear regression analysis indicated concentration dependence. For the MN assay, the conditional binomial test was performed

in Microsoft Excel 2000. The χ^2-test was used to evaluate the statistical significance of the ratio of apoptotic to normal cells. We considered P-values <0.05 as significant. The Dunn test was used for multiple comparisons in the conditional binomial and χ^2-test. SAS, Windows edition (System release 7.10), was used for linear regression analysis and to calculate the IC_{50}.

3. Results

3.1. Cytotoxicity

5-FU was cytotoxic in all cell lines in a concentration-dependent manner (Fig. 1). In MOLY and TK6 cells, there were severe cytotoxicity in the highest dose. The IC_{50} of RS0 was 2.4 μg/mL in MOLY cells, 15.4 μg/mL in TK6 cells, and 30.6 μg/mL in WTK-1 cells.

3.2. Tk assay

5-FU increased MF in MOLY cells in a concentration-dependent manner ($P=0.021$, linear regression analysis), doubling the total MF relative to the solvent control at 2.0 μg/mL and quadrupling it at 4.0 μg/mL (Fig. 1). MF was not increased more than 2 times to the solvent control in TK6 and WTK-1 cells. Therefore 5-FU was not mutagenic to TK6 or WTK-1 cells while MMS, the positive control, was.

3.3. MN assay

5-FU increased the MN frequency to 5.5 times the control value at 2.0 μg/mL ($P=0.0003$) and 14.5 times the control value at 4.0 μg/mL ($P<0.0001$) in MOLY cells in a concentration-dependent manner (Fig. 2). In WTK-1 cells, 5-FU increased the MN frequency to 7.3 times the control value only at 50 μg/mL ($P=0.0001$). 5-FU was not clastogenic in TK6 cells while MMS, the positive control, was.

3.4. Measurement of apoptotic cells

5-FU at the higher concentrations significantly increased the ratio of cells in apoptosis 24 h after treatment in all cell lines ($P<0.0001$–0.0162, χ^2-test) (Fig. 3). TK6 cells showed the greatest response. At the same level of cytotoxicity, the levels of apoptosis in MOLY and WTK-1 cells were similar. We confirmed apoptosis by nuclear morphology analysis.

3.5. Cell cycle effects

Fig. 4 shows the time course of cell cycle distribution following treatment with various concentration of 5-FU. In MOLY cells, no G_2/M phase cells were evident 0.5 h after treatment and G_1 phase cells accumulated slightly. At 24 h, we observed cell cycle delay at 4.0 μg/mL

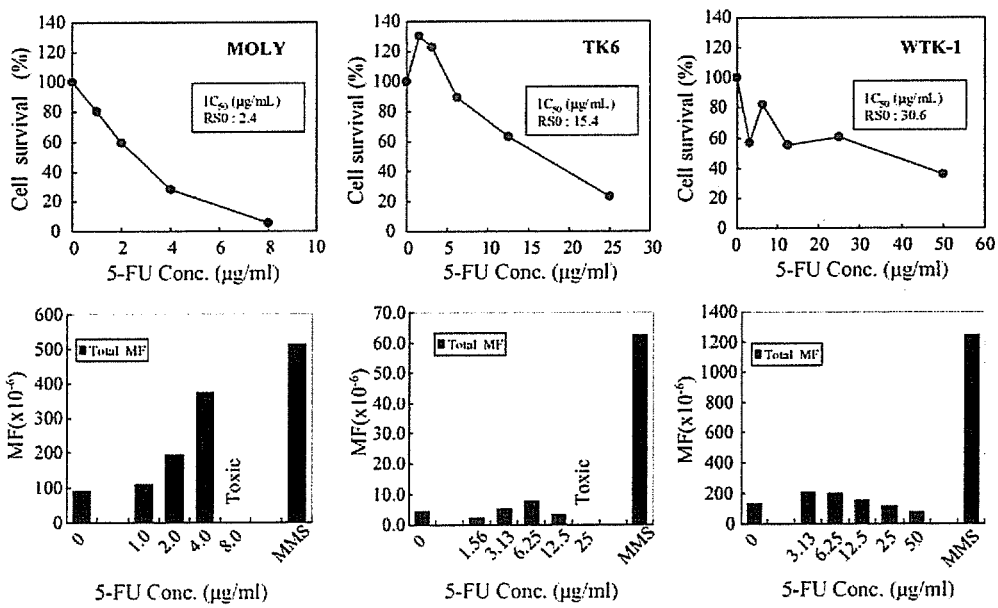

Fig. 1. The mutation frequency and cytotoxicity in tk assay after 5-FU treatment in MOLY, TK6 and WTK-1 cells. The percentage of cell survival (RS0, line graphs) and total MF (bar graphs) after 5-FU treatment (MOLY cells for 3 h and the human cell lines for 4 h) were shown. 5-FU was cytotoxic in all cell lines in a concentration-dependent manner. 5-FU increased MF in MOLY cells in a concentration-dependent manner, however not mutagenic to TK6 or WTK-1 cells.

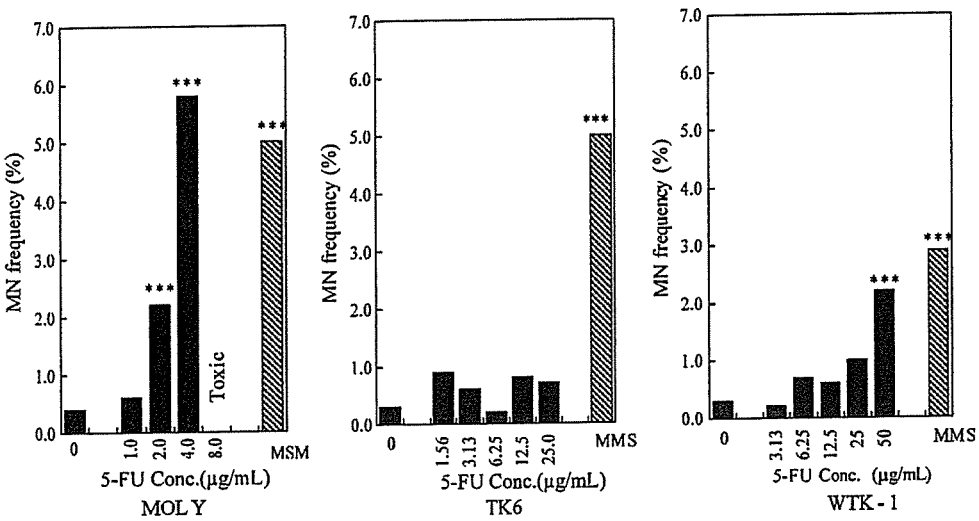

Fig. 2. The frequency of cells with micronuclei in MOLY, TK6 and WTK-1 cells after 5-FU treatment. The frequency of cells with MN (MN frequency) 48 h after 5-FU treatment was shown. One thousand cells from each treatment group were observed and the number with MN was counted. 5-FU significantly increased MN frequency in comparison with the control value at 2.0 ($P = 0.0003$) and 4.0 μg/mL ($P < 0.0001$) in MOLY cells. 5-FU increased MN frequency only at 50 μg/mL ($P = 0.0001$) in WTK-1 cells. 5-FU was not clastogenic in TK6 cells. ***$P < 0.001$, conditional binomial test.

5-FU. The cell cycle returned to normal 48 h after treatment.

In TK6 cells, we observed no cell cycle changes 0.5 h after treatment. G_1 phase cells accumulated in direct proportion to 5-FU concentration 24 h after treatment, and the cell cycle recovered by 72 h. G_2/M phase cells disappeared in the highest dose 24 h after treatment.

WTK-1 cells also underwent no cell cycle changes 0.5 h after treatment. Cells were arrested in S phase 24 h after treatment but recovered by 48 h in all concentration

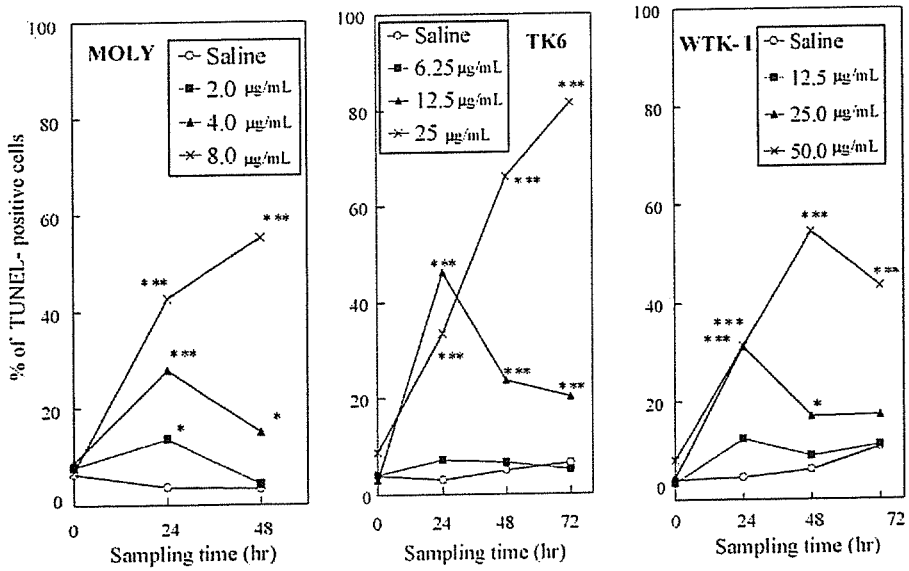

Fig. 3. The percentage of TUNEL-positive MOLY, TK6, and WTK-1 cells after 5-FU treatment. For analysis of apoptosis, 10,000 cells were analyzed at 0.5, 24, and 48 h (all cell lines) or at 72 h (TK6 and WTK-1 cells) after 5-FU treatment. 5-FU increased the ratio of apoptotic cells 24 h after treatment in all cell lines. The ratio of apoptotic cells was the highest in TK6 cells. The levels of apoptosis in MOLY and WTK-1 cells were similar at the same level of cytotoxicity. *$P < 0.05$; ***$P < 0.001$ (relative to saline control); χ^2-test.

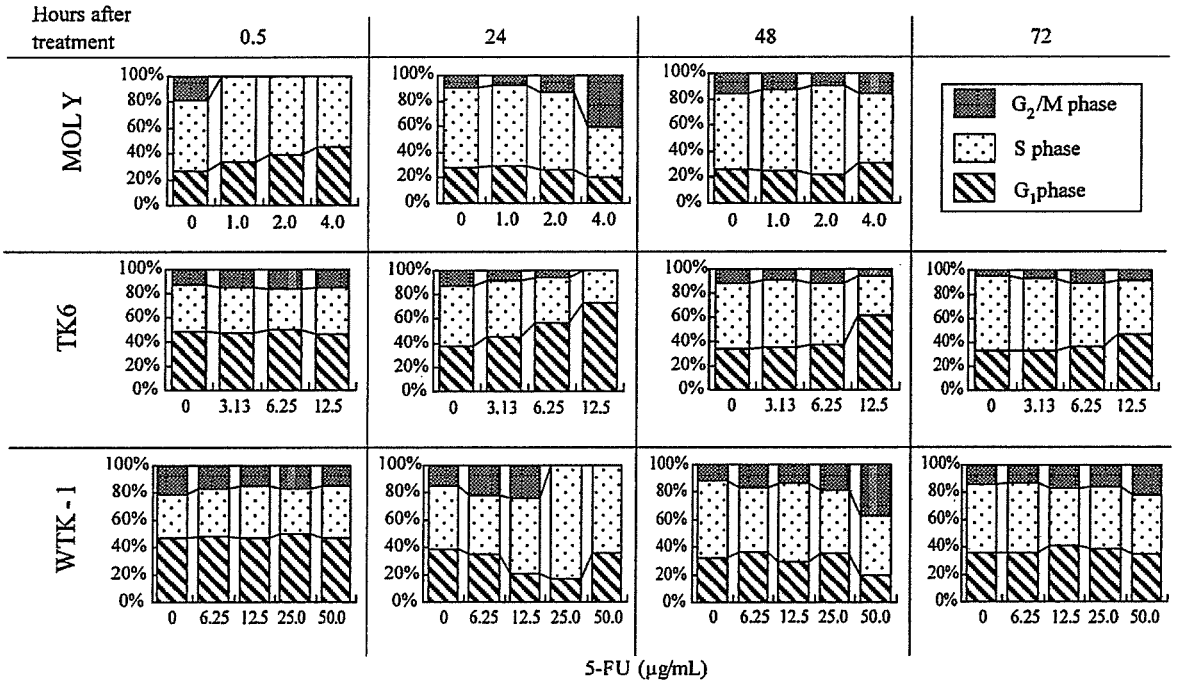

Fig. 4. Time course of cell cycle distribution in MOLY, TK6, and WTK-1 cells following 5-FU treatment. For analysis of cell cycle distribution, 10,000 cells were analyzed at 0.5, 24, and 48 h (all cell lines) or at 72 h (TK6 and WTK-1 cells) after 5-FU treatment. In MOLY cells, no G_2/M phase cells were evident 0.5 h after treatment. At 24 h, the cell cycle delayed at 4.0 μg/mL 5-FU. The cell cycle returned to normal 48 h after treatment. In TK6 and WTK-1 cells, there was no cell cycle change 0.5 h after treatment. G_2/M phase cells disappeared in the highest dose (TK6 cells) and in the higher 2 doses (WTK-1 cells) 24 h after treatment. In TK6 cells, G1 phase cells accumulated in direct proportion to 5-FU concentration 24 h after treatment, and the cell cycle recovered by 72 h. In WTK-1 cells, cells were arrested in S phase 24 h after treatment but recovered by 48 h in all concentration groups.

groups. G_2/M phase cells disappeared in the higher two doses 24 h after treatment.

3.6. Enzyme activity and TS content

Table 1 shows TS content and DPD, OPRT, and TP activity in MOLY, TK6, and WTK-1 cells. The cell lines did not differ much in TS content. MOLY cells showed the highest OPRT activity and the lowest DPD and TP activity. TK6 cells showed lower DPD activity than WTK-1 cells, but the TS content was higher in TK6 cells than in WTK-1 cells.

Table 1
The content and activities of 5-FU related metabolism and catabolism enzymes in MOLY, TK6, and WTK-1 cells

Enzyme (units)	Cell lines		
	MOLY	TK6	WTK-1
TS contents (pmol/min/mg protein)	0.726	1.284	0.573
OPRT activity (pmol/min/mg)	171.8	21.5	39.6
DPD activity (pmol/min/mg)	0.28	10.11	34.97
TP activity (pmol/min/mg)	ND	20.58	16.08

Abbr.: TS, thymidylate synthetase; OPRT, orotate phosphoribosyl transferase; DPD, dihydrouracil dehydrogenase; TP, thymidine phosphorylase; ND, not detected.

4. Discussion

In general, X-rays and mutagens induce more cytotoxicity and/or a higher frequency of apoptosis in cells with wild type p53 and a higher frequency of mutations and chromosomal aberrations in cells with mutant p53 [3]. Because the mutated p53 site in both MOLY (codon 170 of exon 5) and WTK-1 cells (codon 237 of exon 7) are part of the central DNA binding domain [13], and because 5-FU was positive in the *Tk* assay in MOLY cells [5,30], we expected 5-FU to be positive in WTK-1 cells as well. It was not, however, indicating that 5-FU mutagenicity did not depend on p53 function. Furthermore, 5-FU was much more cytotoxic in MOLY cells, which have a mutant p53 gene, than in TK6 cells, which have the wild type p53 gene, indicating that 5-FU cytotoxicity also did not depend on p53 function. At the same level of cytotoxicity, the level of apoptosis was similar in MOLY and WTK-1 cells, suggesting that the induction of apoptosis cells was not directly related to 5-FU muta-

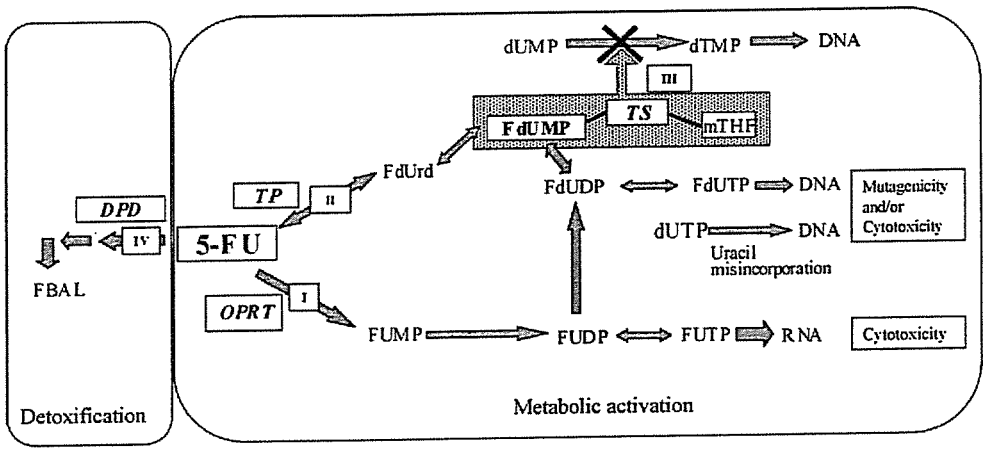

Fig. 5. The intracellular metabolism and catabolism of 5-FU. (I) 5-FU is metabolized by OPRT to FUMP. (II) 5-FU is metabolized to FdUrd by TP, but TP can convert FdUrd to 5-FU. (III) When 5-FU is converted to the active form of 5-FU, FdUMP, it forms complex with TS and 5,10-methylene tetrahydrofolate, and competitively inhibits DNA synthesis. (IV) 5-FU is detoxicated by DPD to FBAL. Thymidine depletion is a trigger for DSBs. DSBs are caused by the misincorporation of dUTP and/or misrepair of the uracil-containing lesion. Furthermore, 5-FU induces DNA strand breaks by the direct incorporation of 5-fluoro-deoxyuridine triphosphate (FdUTP). 5-FU is also misincorporated to RNA, and show the cytotoxicity. Modified from IARC Monographs [26].

genicity in MOLY and WTK-1 cells. Cell cycle analysis showed no clear difference between MOLY cells and the human cell lines, suggesting that p53 gene status did not directly determine the sensitivity of the cells to 5-FU mutagenicity and cytotoxicity.

Fig. 5 shows the intracellular metabolism and detoxification of 5-FU. When 5-FU, a fluorinated pyrimidine base analogue, is converted to 5-fluoro-2-deoxyuridylate monophosphate (FdUMP), it complexes with TS and 5,10-methylene tetrahydrofolate (CH_2FH_4), and competitively inhibits DNA synthesis [23–26]. Thymidine depletion by TS inhibition induces a nucleotide pool imbalance and the misincorporation of dUTP and/or misrepair of the uracil-containing lesion, causing double strand DNA breaks (DSBs) [40–42]. Furthermore, the direct incorporation of 5-fluoro-deoxyuridine triphosphate (FdUTP) inhibits DNA synthesis [24]. Therefore, the intracellular metabolism of 5-FU to FdUMP or FdUTP leads to cytotoxic and mutagenic effects.

5-FU can be metabolized by OPRT to fluoro-uridylate monophosphate and detoxified by DPD to fluoro-β-alanine, or by TP to 5-fluoro-deoxyuridine (FdUrd) and, in turn, back to 5-FU (Fig. 5). In this study, DPD activity was lower and OPRT activity was higher in MOLY cells than in TK6 and WTK-1 cells, suggesting the efficient metabolism of 5-FU in MOLY cells, which could have led to the strong cytotoxic and mutagenic effects that we observed.

Only MOLY cells had no TP activity in this study. TP and OPRT are involved in the intracellular metabolism of 5-FU. Inhibition of OPRT decreases the incorporation of 5-FU into nucleotides and therefore its cytotoxicity, while TP has no effect [43]. Thus, the absence of TP activity in MOLY cells would have little effect on its sensitivity to 5-FU. TS content, on the other hand, was not associated with the cytotoxic and mutagenic effects of 5-FU.

From these findings, we conclude that the difference in DPD and OPRT activity in MOLY, TK6, and WTK-1 cells were responsible for differences in the cells' cytotoxic and mutagenic responses to 5-FU.

The relationship between sensitivity to 5-FU and the intracellular distribution of 5-FU metabolic enzymes indicate that differences in the way that human cells and animal cells metabolize a chemical can cause differences in mutagenicity test results. Thus, potentially mutagenic chemicals should be tested in human cells as well as animal cells.

Compared with WTK-1 cells, TK6 cells had much lower DPD activity, and 5-FU in TK6 cells was efficiently metabolized to FdUMP without being detoxified. But the TS content was higher in TK6 cells than in WTK-1 cells, so 5-FU metabolism would not be very different in TK6 and WTK-1 cells. In this study, however, 5-FU cytotoxicity was higher in TK6 cells than in WTK-1 cells, perhaps because 5-FU is more cytotoxic in p53 normal cells than in p53 mutant or null cells [15–17]. Our results suggest that if 5-FU metabolizing enzyme activity is equivalent, p53 status might influence 5-FU cytotoxicity. Indeed, p53 status might influence responses to cytotoxicity induced by 5-FU as it does to cytotoxicity induced by X-rays [3]. Furthermore 5-FU increased the

MN frequency in MOLY and WTK-1 cells but not TK6 cells, while the ratio of apoptosis cells induced by 5-FU was the highest in TK6 cells. In TK6 cells, the wild type p53 gene might suppress the induction of micronuclei by leading of DNA damaged cells to apoptosis. Thus, 5-FU mutagenicity might be influenced by also the p53 gene status. However, IC_{50} of RS0 was obviously lower and MF was obviously higher in MOLY cells than TK6 and WTK-1 cells. Therefore we suspected that the difference in 5-FU metabolism influenced to 5-FU cytotoxicity and mutagenicity more than the p53 gene status.

In summary, our study showing that MOLY cells were more sensitive than WTK-1 cells to 5-FU cytotoxicity and mutagenicity even though both have a mutated p53 gene suggested that those differences were attributable to differences in 5-FU metabolism rather than the p53 gene status.

Acknowledgments

We thank Drs. Tanaka and Wakuri, Hatano Research Institute, Food and Drug Safety Center, for providing us with MOLY, TK6, and WTK-1 cell lines. We are indebted to Dr. M. Bloom for the precise review of the manuscripts.

References

[1] T.J. Oberly, B.J. Bewsey, G.S. Probst, An evaluation of L5178YTK$^{+/-}$ mouse lymphoma forward mutation assay using 42 chemicals, Mutat. Res. 125 (1984) 291–306.

[2] P. Clay, M.F. Cross, Microwell mutation assays: evaluation of ethyl methanesulfonate, benzo[a]pyrene and benzidine using the tk locus in L5178Y mouse lymphoma cells, Mutagenesis 5 (Suppl.) (1990) 45–54.

[3] M. Honma, M. Hayashi, T. Sofuni, Cytotoxic and mutagenic responses to X-rays and chemical mutagens in normal and p53-mutated human lymphoblastoid cells, Mutat. Res. 374 (1997) 89–98.

[4] M. Honma, L.S. Zhang, M. Hayashi, K. Takeshita, Y. Nakagawa, N. Tanaka, T. Sofuni, Illegitimate recombination leading to allelic loss and unbalanced translocation in p53-mutated human lymphoblastoid cells, Mol. Cell. Biol. 17 (1997) 4774–4781.

[5] M. Honma, M. Hayashi, H. Shimada, N. Tanaka, S. Wakuri, T. Awogi, K.I. Yamamoto, N. Kodani, Y. Nishi, M. Nakadate, T. Sofuni, Evaluation of the mouse lymphoma tk assay (microwell method) as an alternative to the in vitro chromosomal aberration test, Mutagenesis 14 (1999) 5–22.

[6] D. Clive, J.F.S. Spector, Laboratory procedure assessing specific locus mutation at the TK locus in cultured L5178Y mouse lymphoma cells, Mutat. Res. 31 (1975) 17–29.

[7] P.M. Leong-Morgenthaler, C.O.H. Velt, E. Jaccaud, R.J. Turesky, Mutagenicity of 2-amino-3-methylimidazo[4,5-f]quinoline in human lymphoblastoid cells, Carcinogenesis 19 (1998) 1749–1754.

[8] Y.Y. Chuang, Q. Chen, J.P. Brown, J.M. Sedivy, H.L. Liber, Radiation-induced mutations at the autosomal thymidine kinase locus are not elevated in p53-null cells, Cancer Res. 59 (1999) 3073–3076.

[9] R.F. Branda, J.P. O'Neill, E.M. Brooks, L.M. Trombley, J.A. Nicklas, The effect of folate deficiency on the cytotoxic and mutagenic responses to ethyl methanesulfonate in human lymphoblastoid cell lines that differ in p53 status, Mutat. Res. 473 (2001) 51–71.

[10] L. Bassi, M. Carloni, E. Fonti, N.P. de la Pena, R. Meschini, F. Palitti, Pifithrin-alpha, an inhibitor of p53, enhances the genetic instability induced by etoposide (VP16) in human lymphoblastoid cells treated in vitro, Mutat. Res. 499 (2002) 163–176.

[11] S.A. Amundson, F. Xia, K. Wolfson, H.L. Liber, Different cytotoxic and mutagenic responses induced by X-rays in two human lymphoblastoid cell lines derived from a single donor, Mutat. Res. 286 (1993) 233–241.

[12] F. Xia, X. Wang, Y.H. Wang, N.M. Tsang, D.W. Yandell, K.T. Kelsey, H.L. Liber, Altered p53 status correlates with differences in sensitivity to radiation-induced mutation and apoptosis in two closely related human lymphoblast lines, Cancer Res. 55 (1995) 12–15.

[13] S.M. Morris, A role for p53 in the frequency and mechanism of mutation, Mutat. Res. 511 (2002) 45–62.

[14] J.L. Schwartz, R. Jordan, B.A. Sedita, M.J. Swenningson, J.P. Banath, P.L. Olive, Different sensitivity to cell killing and chromosome mutation induction by gamma rays in two human lymphoblastoid cell lines derived from a single donor: possible role of apoptosis, Mutagenesis 10 (1995) 227–233.

[15] D. Arango, G.A. Corner, S. Wadler, P.J. Catalano, L.H. Augenlicht, c-myc/p53 interaction determines sensitivity of human colon carcinoma cells to 5-fluorouracil in vitro and in vivo, Cancer Res. 61 (2001) 4910–4915.

[16] J.L. Grem, K.D. Danenberg, K. Behan, A. Parr, L. Young, P.V. Danenberg, D. Nguyen, J. Drake, A. Monks, C.J. Allegra, Thymidine kinase, thymidylate synthase, and dihydropyrimidine dehydrogenase profiles of cell lines of the National Cancer Institute's Anticancer Drug Screen, Clin. Cancer Res. 7 (2001) 999–1009.

[17] D.B. Longley, J. Boyer, W.L. Allen, T. Latif, P.R. Ferguson, P.J. Maxwell, U. McDermott, M. Lynch, D.P. Harkin, P.G. Johnston, The role of thymidylate synthase induction in modulating p53-regulated gene expression in response to 5-fluorouracil and antifolates, Cancer Res. 62 (2002) 2644–2649.

[18] S.K. Greenwood, M.J. Armstrong, R.B. Hill, C.I. Bradt, T.E. Johnson, C.A. Hilliard, S.M. Galloway, Fewer chromosome aberrations and earlier apoptosis induced by DNA synthesis inhibitors, a topoisomerase II inhibitor or alkylating agents in human cells with normal compared with mutant p53, Mutat. Res. 401 (1998) 39–53.

[19] T. Allio, E.M. Donner, R.J. Preston, A comparison of the roles of p53 mutation and AraC inhibition in the enhancement of bleomycin-induced chromatid aberrations in mouse and human cells, Mutat. Res. 447 (2000) 227–237.

[20] T. Allio, R.J. Preston, Increased sensitivity to chromatid aberration induction by bleomycin and neocarzinostatin results from alterations in a DNA damage response pathway, Mutat. Res. 453 (2000) 5–15.

[21] L.S. Zhang, M. Honma, M. Hayashi, T. Suzuki, A. Matsuoka, T. Sofuni, A comparative study of TK6 human lymphoblastoid and L5178Y mouse lymphoma cell lines in the in vitro micronucleus test, Mutat. Res. 347 (1995) 105–115.

[22] R.D. Storer, A.R. Kraynak, T.W. McKelvey, M.C. Elia, T.L. Goodrow, J.G. DeLuca, The mouse lymphoma L5178Y $Tk^{+/-}$ cell line is heterozygous for a codon 170 mutation in the p53 tumor suppressor gene, Mutat. Res. 373 (1997) 157–165.
[23] A.A. Piper, R.M. Fox, Biochemical basis for the differential sensitivity of human T- and B-lymphocyte lines to 5-fluorouracil, Cancer Res. 42 (1982) 3753–3760.
[24] R.B. Diasio, B.E. Harris, Clinical pharmacology of 5-fluorouracil, Clin. Pharmacokinet. 16 (1989) 215–237.
[25] D.M. Thomas, J.R. Zalcberg, 5-fluorouracil: a pharmacological paradigm in the use of cytotoxics, Clin. Exp. Pharmacol. Physiol. 25 (1998) 887–895.
[26] 5-fluorouracil, IARC Monogr. Eval. Carcinogen. Risk Chem. Hum. 26 (1981) 217–235.
[27] L. Griffiths, I.J. Stratford, Platelet-derived endothelial cell growth factor thymidine phosphorylase in tumor growth and response to therapy, Br. J. Cancer 76 (1997) 689–693.
[28] N. Yajima, K. Kondo, K. Morita, Reverse mutation tests in *Salmonella typhimurium* and chromosomal aberration tests in mammalian cells in culture on fluorinated pyrimidine derivatives, Mutat. Res. 88 (1981) 241–254.
[29] A. Ohuchida, A. Furukawa, J. Yoshida, M. Watanabe, F. Aruga, Y. Miwa, K. Shinkawa, N. Kinae, Micronucleus assays on 5-fluorouracil and 6-mercaptopurine with mouse peripheral blood reticulocytes, Mutat. Res. 278 (1992) 139–143.
[30] T. Sofuni, M. Honma, M. Hayashi, H. Shimada, N. Tanaka, S. Wakuri, T. Awogi, K.I. Yamamoto, Y. Nishi, M. Nakadate, Detection of in vitro clastogens and spindle poisons by the mouse lymphoma assay using the microwell method: interim report of an international collaborative study, Mutagenesis 11 (1996) 349–355.
[31] 5-fluorouracil, IARC Monogr. Eval. Carcinogen. Risk Chem. Hum. (Suppl. 6) (1987) 316–318.
[32] T. Matsushima, M. Hayashi, A. Matsuoka, M. Ishidate, K.F. Miura, H. Shimizu, Y. Suzuki, K. Morimoto, H. Ogura, K. Mure, K. Koshi, T. Sofuni, Validation study of the in vitro micronucleus test in a Chinese hamster lung cell line (CHL/IU), Mutagenesis 14 (1999) 569–580.
[33] Y. Gavrieli, Y. Sherman, S.A. Ben-Sasson, Identification of programmed cell death in situ via specific labeling of nuclear DNA fragmentation, J. Cell Biol. 119 (1992) 493–501.
[34] M. Carbonari, M. Cibati, M. Fiorilli, Measurement of apoptotic cells in peripheral blood, Cytometry 22 (1995) 161–167.
[35] C.P. Spears, A.H. Shahinian, R.G. Moran, C. Heidelberger, T.H. Corbett, In vivo kinetics of thymidylate synthetase inhibition of 5-fluorouracil-sensitive and -resistant murine colon adenocarcinomas, Cancer Res. 42 (1982) 450–456.
[36] T. Takechi, J. Uchida, F.A.M. Fukushima, Enhancing 5-fluorouracil cytotoxicity by inhibiting dihydropyrimidine dehydrogenase activity with uracil in human tumor cells, Int. J. Oncol. 11 (1997) 1041–1044.
[37] F.N. Naguib, M.H. el Kouni, S. Cha, Enzymes of uracil catabolism in normal and neoplastic human tissues, Cancer Res. 45 (1985) 5405–5412.
[38] G.J. Peters, E. Laurensse, A. Leyva, J. Lankelma, H.M. Pinedo, Sensitivity of human, murine, and rat cells to 5-fluorouracil and 5′-deoxy-5-fluorouridine in relation to drug-metabolizing enzymes, Cancer Res. 46 (1986) 20–28.
[39] Y. Maehara, H. Nakamura, Y. Nakane, K. Kawai, M. Okamoto, S. Nagayama, T. Shirasaka, S. Fujii, Activities of various enzymes of pyrimidine nucleotide and DNA syntheses in normal and neoplastic human tissues, Gann 73 (1982) 289–298.
[40] H.A. Ingraham, B.Y. Tseng, M. Goulian, Nucleotide levels and incorporation of 5-fluorouracil and uracil into DNA of cells treated with 5-fluorodeoxyuridine, Mol. Pharmacol. 21 (1982) 211–216.
[41] N.J. Curtin, A.L. Harris, G.W. Aherne, Mechanism of cell death following thymidylate synthase inhibition: 2′-deoxyuridine-5′-triphosphate accumulation, DNA damage, and growth inhibition following exposure to CB3717 and dipyridamole, Cancer Res. 51 (1991) 2346–2352.
[42] R.D. Ladner, The role of dUTPase and uracil-DNA repair in cancer chemotherapy, Curr. Protein Pept. Sci. 2 (2001) 361–370.
[43] M. Fukushima, Y. Murakami, N. Suzuki, K. Aiba, The analysis of the innate pathways of 5-fluorouracil phosphorylation in human gastrointestinal cancer cell lines in vitro and in vivo, Oncol. Rep. 4 (1997) 1189–1194.

Genes and Environment

Vol. 28, No. 1, February, 2006

Characterization of Genotoxicity of Kojic Acid by Mutagenicity in Salmonella and Micronucleus Induction in Rodent Liver

Satoko Ishikawa[1], Yu F Sasaki[2], Satomi Kawaguchi[2], Masataka Mochizuki[1] and Minako Nagao[1]

[1]Kyoritsu University of Pharmacy, Tokyo, Japan
[2]Hachinohe National College of Technology, Aomori, Japan

Genes and Environment, Vol. 28, No. 1 pp. 31–37 (2006)

Regular Article

Characterization of Genotoxicity of Kojic Acid by Mutagenicity in Salmonella and Micronucleus Induction in Rodent Liver

Satoko Ishikawa[1], Yu F Sasaki[2], Satomi Kawaguchi[2], Masataka Mochizuki[1] and Minako Nagao[1,3]

[1]Kyoritsu University of Pharmacy, Tokyo, Japan
[2]Hachinohe National College of Technology, Aomori, Japan

(Received December 19, 2005; Accepted January 16, 2006)

Three lots of kojic acid (KA) which were produced for use as a reagent, food additive and in cosmetics were shown to be mutagenic in *S. typhimurium* TA100 with or without S9 mix, with a specific activity of around 100 revertants per mg of KA. Since there are contradictory reports on genotoxicity of KA, we examined, using HPLC, whether the mutagenicity to *S. typhimurium* is due to KA itself, or due to contaminants present in the KA samples. Although two UV absorbing fractions were separated by HPLC, mutagenicity was detected only in the major fraction and the specific mutagenic activity of KA did not change before and after HPLC separation. The material in the major peak fractions on HPLC was confirmed to be KA by NMR. Thus it was demonstrated that KA itself is mutagenic and no mutagenic contaminants were detected in the three lots of samples. Since KA is known to produce liver tumors in mice, we further examined the genotoxicity of KA in the liver of rodents. KA induced micronuclei (MN) in the regenerating liver of adult mice by its gastric intubation at 1 g per kg body weight. However, no MN were induced in young mice (3 weeks old) without partial hepatectomy. Since it was recently found that KA had no tumor-initiating activity in the liver of mice in a two-step carcinogenicity study, there is no evidence that the genotoxicity detected in the mouse liver is involved in liver carcinogenesis.

Key words: mutagenicity, liver micronuclei, genotoxicity, *S. typhimurium*, kojic acid.

Introduction

Kojic acid (KA) [5-hydroxy-2-hydroxymethyl]-4*H*-pyran-4-one; CAS No. 501-30-4; (Fig. 1)] is a natural substance produced by various fungi, *Penicillium* spp., *Aspergillus orizae, flavus and lamarii*, and also by certain bacteria (1). KA which had been used as a food additive for the prevention of enzymatic browning of shell fish, raw crabs and shrimp, owing to its inhibitory activity on tyrosinase, was found to be genotoxic *in vitro*, inducing *his*$^+$ reverse mutations in *S. typhimurium* (2–5). It was also found to be genotoxic *in vivo*, inducing micronuclei (MN) in peripheral blood of rats (6).

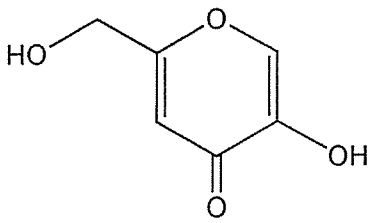

Fig. 1. Structure of kojic acid (KA).

KA had been reported to induce hepatomas and thyroid adenomas in mice (7). Thyroid adenomas or hyperplasia production in the mouse or rat was suggested to be due to promoting activity of KA (7–9). In contrast, the possibility of involvement of genotoxicity of KA in mouse hepatoma development could not be excluded (10). In 2003, the Ministry of Health, Labour and Welfare, Japan noticed that KA was no longer used for prevention of browning of shell fish in market due to the development of modern technology, and KA was withdrawn from the list of existing food additives in the same year. Since KA is a fungal product, soy sauce, miso and sake were suspected to contain KA. Out of 32 samples of fermented foods examined for the presence of KA, three samples were found to be positive, but the levels were not so high, being at the maximum, 1 ppm (personal communication by Dr. Tamio Maitani, National Health Sciences, Tokyo, Japan, Dec. 7, 2005). Further, KA is still used in cosmetics as a skin lightening agent (quasi-drug) at concentrations of up to 1.5% due

[3]Correspondence to: Minako Nagao, Kyoritsu University of Pharmacy, 1-5-30 Shibakoen, Minato-ku, Tokyo 105–8512, Japan. Tel: +81-3-3434-6241, Fax: +81-3-3434-5343, E-mail: mnagao@m8.dion.ne.jp

to its inhibiting action on human melanocyte tyrosinase (11). Thus, the safety of KA needs to be confirmed from various points.

Recently, results of an extensive study on genotoxicity of KA have been reported, in which KA showed only weak mutagenicity without a dose-dependent response in *S. typhimurium* (12). Many contradictory or inconsistent results had been reported for the genotoxicity of KA. KA induced MN in peripheral blood, but not in the liver of young rats by a single application through gastric intubation (6). However, it did not induce MN in bone marrow of mice (12,13) by a single application through intraperitoneal injection. Furthermore, MN were not induced in human keratinocytes SVK14 nor in human hepatocellular carcinoma cells, HepG2, *in vitro* (12) but were induced in human lymphoblastoid cells, TK6 and WTK-1 (personal communication by Dr. Masamitsu Honma, National Institute of Health Sciences, Tokyo Japan, December 12, 2005). KA did not induce $HPRT^-$ mutations in Chinese hamster V79 cells or mouse L5178Y cells (12), but induced TK^- mutation in TK6 ($TK^{+/-}$) and WTK-1 ($TK^{+/-}$, $P53^{-/-}$) cells (unpublished observations, Yu F Sasaki). As for chromosome aberrations and sister chromatid exchanges *in vitro*, positive results were reported in Chinese hamster cells (5).

Since there had been no standards for composition of KA in food hygiene law, while the manufacturers' specifications for cosmetic use was at least 97% pure, there was a possibility that the discordance reported for genotoxicity was due to differences in composition of KA samples used. Thus, it is important to clarify whether the mutagenicities of some KA samples were due to KA itself or contaminant included. In the present study, samples of various lots of KA produced by different companies that are used as a food additive, reagent and cosmetics ingredient were purified by HPLC. The resulting fractions were tested in order to determine whether the reported mutagenicity in *S. typhimurium* was due to KA itself or to another component present in the KA samples. This testing showed that the mutagenicity is due to KA itself and not to contaminants. As KA has been reported to be hepatocarcinogenic in mice (7), we further examined whether KA shows *in vivo* genotoxicity in rodent liver, by MN assay.

Materials and Methods

Chemicals: Kojic acid, reagent grade, lot no. 052K2516 was purchased from Sigma (St. Louis), 5312 used for food additive (content is 100.6%) was supplied from Alps Pharmachemical Industry (Gifu, Japan) and 2Y181 [at least 97% pure, but more typically (by HPLC) was >99% pure] used for cosmetics was supplied from Sansho Seiyaku Co., Ltd (Fukuoka, Japan). For *in vivo* genotoxicity studies, KA for food additive provided by Alps Pharmachemical Industry was used. Cyclophospamide, diethylnitrosamine (DEN), dimethyl sulfoxide (DMSO), 4-nitroquinoline 1-oxide and trifluoroacetic acid were purchased from Wako Pure Chemical Industries (Osaka, Japan), and 1,2-dimethylhydrazine (1,2-DMH) and benzo[*a*]pyrene were from Tokyo Kasei Kogyo (Tokyo, Japan). Solutions of KA were prepared immediately before use.

HPLC separation: Analytical HPLC was performed under three systems. System 1; an LC-20A series from Shimadzu Co. (Kyoto, Japan) equipped with Shimadzu SPD-M20A photodiode detector. A Mightysil RP-18 GP column (5 μm particle, 3 mm i.d. $\times$50 mm; Kanto Chemical Co., Tokyo, Japan) was used at 40°C, with an isocratic eluent of methanol-0.05 % v/v trifluoroacetic acid (3:97) and a flow rate of 0.15 mL/min: System 2; a Shimadzu LC-10A series was used with a Mightysil RP-18 GP column (5 μm particle, 4.6 mm i.d. $\times$250 mm), an eluent of methanol-0.05 % v/v trifluoroacetic acid (3:97) and a flow rate of 0.7 mL/min: System 3; the same equipment and column with system 2, but the eluent used was 0.1% propionic acid-0.05N perchloric acid and a flow rate of 0.7 mL/min. Preparative HPLC was performed on an LC-8A series from Shimadzu Co., using a large volumetric flow cell in the UV detector. A Mightysil RP-18 GP column (5 μm particle, 10 mm i.d. $\times$250 mm; Kanto Chemical Co., Tokyo, Japan) and an eluent of methanol-0.05 % v/v trifluoroacetic acid (3:97) were used with a flow rate of 4.0 mL/min. After separation, each fraction was lyophilized and weighed. All fractions were subjected to mutagenicity testing.

NMR analysis: ^1H and ^{13}C spectra were recorded on an ECP-600 spectrometer (JEOL Ltd., Akishima, Tokyo) using DMSO-d_6 as a solvent.

Mutagenicity assay: The mutation assays were performed using *S. typhimurium* TA100 with and without S9 mix (14). The S9 purchased from Oriental Yeast Co. Ltd (Tokyo, Japan) was prepared from Crj:CD (SD), male rat treated with phenobarbital and 6-naphthoflavone. KA was dissolved in 0.1 mL of distilled water and the assay was performed by the method of preincubation (15). For the mutagenicity test, after separation of samples by HPLC, 1 mg of dried residues was applied to a plate for each of fractions 6, 8 and 9. For fraction 7, a dose-dependent response with 0.5, 1.0 and 1.5 mg/plate was examined and the specific activity was calculated based on the linear regression of the least square method. For other fractions, the residues were dissolved in 500 μL water, and 10 or 100 μL were applied to each plates. Statistic analysis was performed by multiple regression analysis.

Animal and KA administration: Male ddY mice of 3 and 8 weeks old, and male Fischer 344 rats of 8 weeks

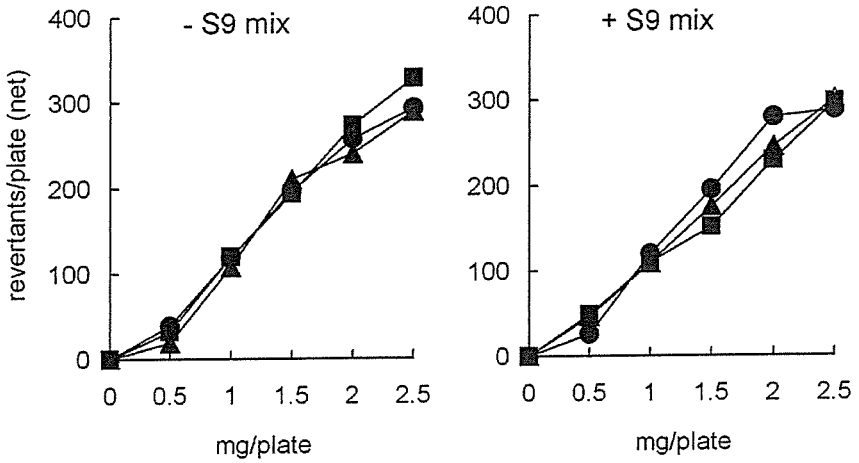

Fig. 2. Mutagenicities of kojic acid (KA) in *S. typhimurium* TA 100 in the absence (left) or presence (right) of S9 mix. The values were averages of two plates, subtracted with numbers of spontaneous revertants of 128 (−S9 mix) or 167 (+S9 mix). Positive control, 0.03 μg of 4-nitroquinoline 1-oxide induced 400 revertants (−S9 mix) and 5 μg of benzo[*a*]pyrene induced 1545 revertants (+S9 mix) over spontaneous one. No statistic differences were observed among these three samples. ●; lot.052K2516, ■; lot.5312, ▲; lot.2Y181.

old were purchased from SLC Japan (Shizuoka, Japan). Eight week old animals were acclimatized for one week at 24±2°C with a relative humidity of 55±5%, with basal diet of MF pellets (Oriental Yeast Industries, Tokyo, Japan) and tap water ad libitum, and were used at age 9 weeks. Three week old mice were used immediately. For gastric intubation, KA was suspended at 0, 50 and 100 mg/mL in 0.5% sodium carboxymethyl-cellulose and immediately administered to animals at a dose of 10 mL/kg, corresponding to KA doses of 0, 500 and 1000 mg/kg. The doses administered to the animals were based on the approximate maximum tolerated dose for each species determined by simple acute toxicity experiments: oral gavage with 2000 mg/kg KA resulted in death of 4/4 mice and 4/4 rats within 3h.

Micronucleus assay: Four mice and rats were used for each KA-dose group and three for positive control groups, following the reported method (16,17). Twenty-four hours after administration of KA, partial hepatectomy (two-thirds) was performed on 9 week old animals by removing three major lobes of the liver, the left lateral, left medial and the right lateral lobes under ether-anesthetized conditions. After four days, the animals were anesthetized with ether, and their livers were perfused *in situ* for 5 min with Liver Perfusion Medium [Hanks' balanced salt solution (Ca^{2+}/Mg^{2+} free) containing 0.5 mM EGTA and 10 mM HEPES (pH 7.2-7.3)] (GIBCO-Invitrogen, Carlsbad, CA), followed by 5 min with Liver Digest Medium (Hanks' balanced solution (Ca^{2+}/Mg^{2+} free) containing 0.05% collagenase type IV, 50 μg/mL trypsin inhibitor, 10 mg/mL bovine serum albumin, 10 mM HEPES, and 560 μg/mL $CaCl_2$) (GIBCO-Invitrogen). Both solutions were maintained at 37°C and delivered at a flow rate of 14 mL/min. The perfused livers were minced in a Petri dish containing Liver Digest Medium; the minced tissue was then passed through gauze, centrifuged at 200 g for 1 min, and the cell pellet obtained was fixed with 1 mL of 10% neutral formaldehyde. Ten μL of the cell suspension were mixed with 10 μL of 500 μg/mL acridine orange, the mixture placed on a glass slide and covered with a coverslip. The number of micronucleated hepatocytes (MNHEPs) among 1000 hepatocytes was recorded for each animal under a fluorescence microscope (×400 or greater), with a blue excitation filter and a yellow barrier filter. MNHEP was defined as a hepatocyte with two nuclei, one being less than 1/4 in diameter of the other nucleus. For 3 week old mice, MN assays were performed by the same procedure without partial hepatectomy, and livers were removed at 72, 96 and 120 h. The differences between the frequencies of MN in KA treated and KA 0 control animals were analyzed by one-way ANOVA followed by pairwise comparisons using the Dunnett test. A P-value of less than 0.05 was considered statistically significant.

All animal experiments were carried out following the guidelines set out by Hachinohe National College of Technology in the Guide for the Care and Use of Laboratory Animals.

Results

Mutagenicity in *S. typhimurium* of KA for reagent, food additive and cosmetics: Three lots of KA, 052K2516 (reagent), 5312 (food additive) and 2Y181 (cosmetics) showed similar mutagenic activities in TA 100, under conditions without or with S9 mix (Fig. 2). All samples showed linear dose-dependent response between 0.5 and 1.5 mg/plate of KA. The specific mutagenic activities calculated by linear regression by

Table 1. Weight and mutagenicity in *S. typhimurium* TA100 of each fraction obtained by HPLC of KA samples

Fr. No.	Lot. 052K2516			Lot. 5312			Lot. 2Y181		
	Weight (mg/Fr.)	Revertants/Fr.		Weight (mg/Fr.)	Revertants/Fr.		Weight (mg/Fr.)	Revertants/Fr.	
		−S9 mix	+S9 mix		−S9 mix	+S9 mix		−S9 mix	+S9 mix
1	0.2	0	0	0.6	0	20	0.1	0	0
2	0.2	0	0	0.4	0	0	0.1	0	0
3	0.2	0	0	0.3	0	0	0.0	0	0
4	0.2	0	0	0.4	0	0	0.1	0	0
5	0.0	0	0	0.0	0	30	0.1	0	0
6	11.3	1402	1232	14.2	2321	1734	10.2	1129	946
7	22.8	2686	3051	27.0	4260	3504	33.4	3176	3377
8	15.1	1595	1700	17.4	2153	2205	26.6	2258	2471
9	7.4	749	853	9.0	945	1359	11.6	1170	961
10	2.9	292	213	2.3	259	94	4.1	410	250
11	2.0	0	0	0.3	25	0	1.2	0	0
12	0.8	0	0	0.3	85	0	0.2	0	0
13	0.4	0	0	0.4	85	0	0.2	0	0
14	0.4	0	0	0.1	40	0	0.2	0	0
Total weight	63.9			72.5			88.1		

the least square method for 052K2516, 5312 and 2Y181 were 116, 115 and 106 revertants/mg, respectively, without S9 mix and 113, 106 and 111, respectively, with S9 mix. No statistic differences were detected among these different sources of samples at significance of ≤ 0.05.

Separation of mutagenic substance in KA samples by HPLC: To clarify whether the mutagenicity was derived from KA itself or some contaminants in the samples, HPLC separations were performed. A KA sample solution in distilled water of 0.5 μg/0.5 μL was eluted by analytical HPLC under the conditions described in Materials and Methods (systems 1–3). The chromatograms under system 1 of three lots of KA monitored by absorption at 270 nm were similar, and revealed a single peak at 3.8 min (Fig. 3a). Only when a very large amount of KA was applied, a small shoulder peak was detected at the foot of the major peak (data not shown). Using two other different HPLC systems 2 and 3, similar chromatograms were obtained with three samples of KA (data not shown), with their small and very large amounts. These results indicated only a minor UV absorbing material(s) are contaminated in all three samples at similar levels.

Preparative HPLC was then applied to each lot of KA to facilitate the determination of the mutagenicity of the various constituents of the KA samples. A 500 μL aliquot of 25 mg/mL KA solution in distilled water was applied to a column, under the conditions described in Materials and Methods. Typical 270 nm chromatograms of the three samples are shown in Fig 3b. From the chromatograms, it can be seen that all of the samples include an impurity detected as a small peak shoulder, which was eluted after the major peak (arrows in Fig 3b). Circa 100 mg of each KA sample was separated by repeating the HPLC eight times, then all corresponding fractions of the eight runs were pooled and lyophilized to dryness. The contaminant distributed in fractions 10 and 11 in all three samples. The residual weight of each fraction (Table 1) correlated well with its absorption at 270 nm (Fig 3b).

When each fraction was examined for mutagenicity in *S. typhimurium* TA100, fractions 6–10 of all three samples were mutagenic with and without S9 mix, while no significant mutagenicity was detected in the other fractions, under either condition. The total mutagenicity of each fraction of the three samples (Table 1) correlated well with its absorption at 270 nm (Figs 3). All three lots of KA supplied were slightly colored, but after preparative HPLC, the purified KA (fractions 6–9) was almost colorless, and fractions 10 and 11 were strongly colored according to the original color shade.

Table 2 shows the specific activities (revertants/mg) of fractions 6–10. Since fraction 10 contained significant amounts of contaminant, the average specific activities of fractions 6–9 of each sample are also indicated, together with those of the original KA samples, calculated from the data presented in Fig 2, by linear regression by least square method. The specific activities of the three samples were almost the same before and after separation by HPLC, with and without S9 mix.

Structure confirmation by NMR: The dried residues of fractions 6–9 of 052K165, 5312 and 2Y181 were subjected to ^{1}H and ^{13}C-NMR analysis. All of the protons in the KA structure (Fig. 1) were detected in the ^{1}H-NMR spectra, with the following chemical shifts; 4.29 (doublet, CH_2), 5.65 (triplet, CH_2-OH, exchanges with D_2O), 6.33 (singlet, 5-H), 8.02 (singlet, 2-H), and

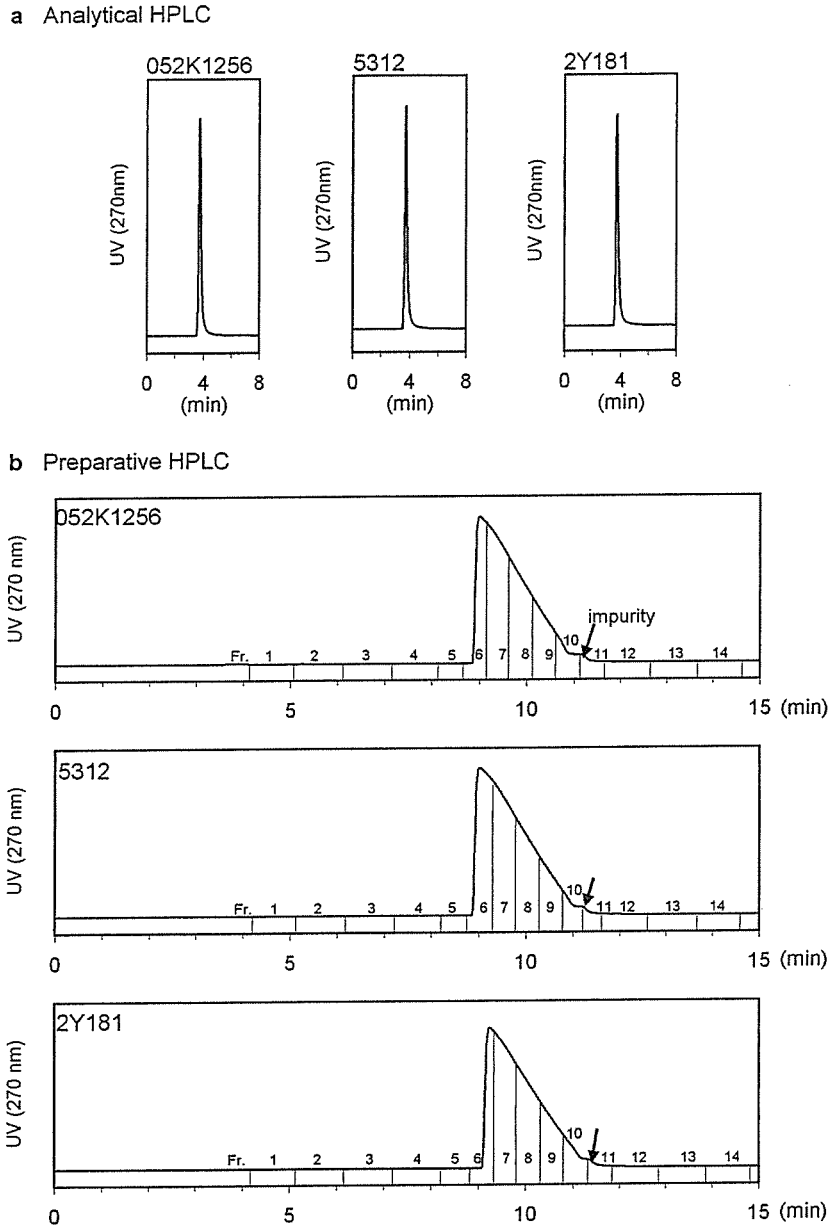

Fig. 3. Analytical (a) and preparative HPLC chromatograms (b) of three samples of KA (lot. 052K1256, 5312, 2Y181) (a): A 0.5 μL aliquot of KA solution (1 mg/mL) in distilled water was loaded on an analytical column (Mightysil RP-18 GP, 3 × 50 mm), and separated by an eluent of methanol − 0.05 v/v% trifluoroacetic acid (3:97) with a flow rate of 0.15 mL/min and absorption at 270 nm was recorded. (b): A 500 μL aliquot of KA solution (25 mg/mL) was applied to a preparative column, Mightysil RP-18 GP (5 μm, 10 × 250 mm), and separated by the same eluent as that used for analytical HPLC with a flow rate of 4 mL/min. In addition to the major peak of KA, a small shoulder peak of impurity was detected as indicated by arrow.

9.05 (singlet, C=C-OH, exchanges with D_2O) ppm. Further, the KA carbon skeleton was detected by ^{13}C-NMR at 60.01 (exocyclic carbon ($\underline{C}H_2$)), 110.37 (C3), 139.79 (C6), 146.25 (C5), 168.61 (C2), and 176.09 (C4(C=O)) ppm. No impurity peaks were detected in any of the samples analyzed. Thus, the major 270 nm absorbing substances in these three samples were confirmed to be KA (data not shown).

***In vivo* genotoxicity of KA:** *In vivo* genotoxicity of KA was examined by MN assay in regenerating livers of mice and rats. Four days after partial hepatectomy (120 h after KA administration), mean values of MNHPCs in mice increased dose dependently and with 1000 mg/kg of KA, the value was significantly increased as compared with 0 dose of KA (Table 3). In rats, however, no increase was observed. Furthermore, KA was found to have no MN inducing ability in infant mice without partial hepatectomy (3 weeks old) (Table 4).

Table 2. Specific mutagenicity in *S. typhimurium* TA100 of KA samples after HPLC separation

Fraction No.	Revertants/mg					
	Lot. 052K1652		Lot. 5312		Lot. 2Y181	
	−S9 mix	+S9 mix	−S9 mix	+S9 mix	−S9 mix	+S9 mix
6	124	109	164	120	111	93
7	118	134	158	130	95	101
8	106	113	124	127	85	93
9	101	115	105	151	101	83
10	95	71	113	41	128	76
Average ± SEM*	112 ± 5.3	118 ± 5.6	138 ± 14	132 ± 6.7	98 ± 5.4	93 ± 3.7
Before HPLC**	116	113	115	106	106	111

Fractions 6, 8 and 9 were analyzed with 1 mg/plate of dried substance. Fraction 7 was tested with 0.5, 1.0 and 1.5 mg/plate of the dried substance, specific mutagenicity was calculated from the linear regression by the least square method. Other fractions were tested with 2 and 20% of dried substances, and results of tests with 20% of total residue of each fraction are indicated. With 2% weight of each fraction, no more than 20% of spontaneous mutagenicity was detected. For fraction 10, the mg amount applied to a plate is; lot.052K1652, 0.58 mg; lot. 5312, 0.46 mg; lot. 2Y181, 0.64 mg. Means of duplicate assays are indicated.

*Average of specific activities of fractions 6~9 ± standard error of means (SEM).
**Values were calculated from Fig. 2, based on the linear regression by the least square method.

Table 3. MN induced in regenerating liver of mice and rats treated with single gavages of KA

Species	Chemical	Dose (mg/kg)	MNHPCs/1000 HPCs (mean ± SEM)
Mouse	KA	0	2.33 ± 0.33
		500	5.00 ± 1.00
		1000	10.3 ± 1.45*
	DEN	160	15.7 ± 1.20*
Rat	KA	0	1.67 ± 0.33
		500	2.00 ± 0.58
		1000	1.33 ± 0.33
	DEN	160	17.3 ± 2.01*

KA, kojic acid; DEN, diethylnitrosamine
MNHPCs, micronucleated hepatocytes; HPCs, hepatocytes.
*Significantly different from control: $p < 0.05$.

Table 4. Micronuclei induced by KA in the liver of young mice

Chemical	Dose (mg/kg)	MNHPCs/1000HPCs (Mean ± SEM)		
		72 h	96 h	120 h
KA	0	0.75 ± 0.48	1.75 ± 0.75	1.5 ± 0.65
	500	0.75 ± 0.25	2.00 ± 0.82	1.75 ± 0.75
	1000	2.00 ± 0.41	2.00 ± 0.41	2.75 ± 0.75
Cyclophosphamide	20		8.75 ± 1.38*	

MNHPCs, micronucleated hepatocytes; HPCs, hepatocytes.
*Significantly different from KA 0 control: $p < 0.05$ by student *t* test.

Discussion

In the present study, KA samples used as a reagent, food additive and cosmetics ingredient showed mutagenicity in *S. typhimurium* TA100. The mutagenic activities of the samples were almost the same with or without S9 mix. The specific activity was weak, being around 100 revertants per mg (Table 2). The major, 270 nm absorbing component of each sample was isolated by preparative HPLC at a retention time of 8.5–10.5 min (Fig. 3b) and identified as KA by NMR analysis. Each KA sample supplied contained some UV absorbing materials which eluted later than KA (indicated by arrow in Fig. 3b). However, the impurity fraction, fraction 11, did not show any mutagenicity. When the mutagenic activities per unit weight of the three lots of KA supplied are compared with those of the major peak fractions 6–9 obtained by HPLC separation, there are no appreciable differences (Table 2). Although preparation methods of these three KA samples supplied are not available, features of these three samples are different and it is suspected that their preparation methods are different. Although a possibility of contamination of mutagenic non-UV absorbing material(s) which behave in the same way as KA on HPLC could not be completely negated, this possibility can be expected as negligible. Thus, it is indicated that all three lots did not contain mutagenic contaminants, and the mutagenic activity of the KA samples is solely derived from KA.

KA, at a dose of 1 g/kg, induced MN in the regenerating liver of mice. Thus, it seems that KA is genotoxic to liver. However this genotoxicity of KA was not detected in the liver of infant mice, on which partial hepatectomies were not performed. The reason for not detecting genotoxicity of KA in infant mice might have been because, while the mitotic index is expected to rise to a very high level after partial hepatectomy, it would be much lower in infant mice (3 weeks old). Further, differences in the metabolisms of infant mice and adult mice having received partial hepatectomies may play

some roles in this difference in genotoxicity (18). It is also noteworthy that KA did not induce MN in bone marrow of mice (12,13).

In contrast, KA was not genotoxic in regenerating rat's liver (Table 3). KA was also recently reported by Suzuki *et al.* (6). not to induce MN in young rats (4 weeks old). However, KA induced MN in peripheral blood of young rats (6). At present, neither the molecular mechanism of the genotoxicity of KA, nor the difference in metabolisms between rats and mice is known.

During preparation of this manuscript it has been reported in a two step carcinogenesis study, in which mice were fed a diet containing 3% KA at initiation step and phenobarbital was used as a tumor promoter, that there is no liver tumor initiating activity (19). At present, it is not clear whether the partial hepatectomy which was performed two weeks after the beginning of phenobarbital administration was at an appropriate time to detect initiating activity of KA or not. It is possible that the difference in the timing of the partial hepatectomy after cessation of KA administration might be one of the reasons for the discrepancy between KA being positive in MN induction and negative in initiating activity.

Although in the present study, genotoxicity of KA was detected in the mouse liver, it was not proved that this genotoxicity is involved in hepatic tumor development in mice.

Acknowledgement: Dr. Makoto Hayashi of National Institute of Health Sciences is thanked for his critical reading of this manuscript. This study was supported by Grants-in-Aid for the Health and Labour Sciences from the Ministry of Health, Labour and Welfare, Japan.

References

1 Manabe M, Goto T, Tanaka K, Matsuura S. The capabilities of the *Aspergillus flavus* group to produce aflatoxins and kojic acid. Rept Natl Food Res Inst. 1981; 38: 115–20 (Japanese).

2 Wehner FC, Thiel PG, van Rensburg SJ, Demasius IP. Mutagenicity to *Salmonella typhimurium* of some *Aspergillus* and *Penicillium* mycotoxins. Mutat Res. 1978; 58: 193–203.

3 Shibuya T, Murota T, Sakamoto K, Iwahara S, Ikeno M. Mutagenicity and dominant lethal test of kojic acid–Ames test, forward mutation test in cultured Chinese hamster cells and dominant lethal test in mice. J Toxicol Sci. 1982; 7: 255–62.

4 Bjeldanes LF, Chew H. Mutagenicity of 1,2-dicarbonyl compounds: maltol, kojic acid, diacetyl and related substances. Mutat Res 1979; 67: 367–71.

5 Wei CI, Huang TS, Fernando SY, Chung KT. Mutagenicity studies of kojic acid. Toxicol Lett. 1991; 59: 213–20.

6 Suzuki H, Ikeda N, Kobayashi K, Terashima Y, Shimada Y, Suzuki T, Hagiwara T, Hatakeyama S, Nagaoka K, Yoshida J, Saito Y, Tanaka J, Hayashi M. Evaluation of liver and peripheral blood micronucleus assays with 9 chemicals using young rats. A study by the Collaborative Study Group for the Micronucleus Test (CSGMT)/ Japanese Environmental Mutagen Society (JEMS)-Mammalian Mutagenicity Study Group (MMS). Mutat Res. 2005; 583: 133–45.

7 Fujimoto N, Watanabe H, Nakatani T, Roy G, Ito A. Induction of thyroid tumours in (C57BL/6N× C3H/N)F1 mice by oral administration of kojic acid. Food Chem Toxicol. 1998; 36: 697–703.

8 Fujimoto N, Onodera H, Mitsumori K, Tamura T, Maruyama S, Ito A. Changes in thyroid function during development of thyroid hyperplasia induced by kojic acid in F344 rats. Carcinogenesis. 1999; 20: 1567–71.

9 Mitsumori K, Onodera H, Takahashi M, Funakoshi T, Tamura T, Yasuhara K, Takegawa K, Takahashi M. Promoting effects of kojic acid due to serum TSH elevation resulting from reduced serum thyroid hormone levels on development of thyroid proliferative lesions in rats initiated with N-bis(2-hydroxypropyl)nitrosamine. Carcinogenesis. 1999; 20: 173–6.

10 Takizawa T, Mitsumori K, Tamura T, Nasu M, Ueda M, Imai T, Hirose M. Hepatocellular tumor induction in heterozygous p53-deficient CBA mice by a 26-week dietary administration of kojic acid. Toxicol Sci. 2003; 7: 3287–93.

11 Maeda K, Fukuda M. *In vitro* effectiveness of several whitening cosmetic components in human melanocytes. J Soc Cosm Chem. 1991; 42: 361–8.

12 Nohynek GJ, Kirkland D, Marzin D, Toutain H, Leclerc-Ribaud C, Jinnai H. An assessment of the genotoxicity and human health risk of topical use of kojic acid [5-hydroxy-2-(hydroxymethyl)-4*H*-pyran-4-one]. Food Chem Toxicol. 2004; 42: 93–105.

13 Nonaka M, Omura H, Sofuni T, Hayashi M. Kojic acid did not induce micronuclei in mouse bonemarrow hematopoietic cells. MMS Commun. 1996; 4: 109–12.

14 Maron DM, Ames BN. Revised methods for the Salmonella mutagenicity test. Mutat Res. 1983; 113: 173–215.

15 Yahagi T, Nagao M, Seino Y, Matsushima T, Sugimura T, Okada M. Mutagenicities of N-nitrosamines on Salmonella, Mutat Res. 1977; 48: 121–30.

16 Suzuki H, Shirotori T, Hayashi M. A liver micronucleus assay using young rats exposed to diethylnitrosamine: methodological establishment and evaluation. Cytogenet Genome Res. 2004; 104: 299–303.

17 Parton JW. Garriott ML, An evaluation of micronucleus induction in bone marrow and in hepatocytes isolated from collagenase perfused liver or from formalin-fixed liver using four week-old rats treated with known clastogens. Environ Mol Mutagen. 1997; 29: 379–85.

18 Rossi AM, Romano M, Zaccaro L, Pulci R, Salmona M. DNA synthesis, mitotic index, drug-metabolising systems and cytogenetic analysis in regenerating rat liver. Comparison with bone marrow test after '*in vivo*' treatment with cyclophosphamide. Mutat Res. 1987; 2: 75–82.

19 Moto M, Mori T, Okamura M, Kashida Y, Mitsumori K. Absence of liver tumor-initiating activity of kojic aid in mice. Arch Toxicol. 2005; Oct 18 Epub ahead of print.

Metabolic Enzyme Induction by HepG2 Cells Exposed to Oxygenated and Nonoxygenated Polycyclic Aromatic Hydrocarbons

Kentaro Misaki,†,‡ Saburo Matsui,‡ and Tomonari Matsuda*,‡

Department of Environmental Engineering and Graduate School of Global Environmental Studies, Kyoto University, Yoshidahonmachi, Kyoto 606-8501, Japan

Received August 18, 2006

Oxygenated polycyclic aromatic hydrocarbons (oxy-PAHs) such as polycyclic aromatic quinones and polycyclic aromatic ketones as well as polycyclic aromatic hydrocarbons (PAHs) are abundant in the atmospheric environment. In this study, mRNA induction of six metabolic enzymes including P4501A1, 1A2, and 1B1, aldo-keto reductase 1C1 (AKR1C1), NAD(P)H-dependent quinone oxidoreductase 1 (NQO1), and glutathione S-transferase M1 (GSTM1) were examined in detail in human hepatoma (HepG2) cells exposed to environmentally relevant 13 PAHs and seven oxy-PAHs. Most PAHs such as benzo[*a*]pyrene (B[*a*]P) showed significant induction of P4501A1 and 1A2 mRNA, while induction by oxy-PAHs such as 5,12-naphthacenequinone (NCQ) and 11*H*-benzo[*b*]fluoren-11-one (B[*b*]FO) occurred less strongly. AKR1C1 mRNA was significantly induced by oxy-PAHs, 11*H*-benzo[*a*]fluoren-11-one (B[*a*]-FO), NCQ, cyclopenta[*cd*]pyren-3(4*H*)-one (CPPO), and B[*b*]FO and also by P450s-inducing PAHs such as B[*a*]P, benzo[*k*]fluoranthene (B[*k*]FA), and dibenz[*a,h*]anthracene (DB[*a,h*]A). Both chemical-dependent and time-dependent induction patterns of NQO1 mRNA were of the mixed types of P4501A1 and AKR1C1. The tendency for the decrease of GSTM1 mRNA was observed when exposed to PAHs B[*a*]P and B[*k*]FA.

Introduction

In various atmospheric and aquatic environments, polycyclic aromatic hydrocarbons (PAHs)[1] originally derived from oil fuel and its combustion are detected at high levels (*1*−*4*), and wildlife and humans have risk of exposure. Many studies in regard to PAH mutagenicity, carcinogenicity, and DNA adduct formation have been reported (*5*−*9*). According to the U.S. Environmental Protection Agency and the International Agency for Research on Cancer (IARC), PAHs such as benzo[*a*]pyrene (B[*a*]P), benz-[*a*]anthracene (B[*a*]A), chrysene (Chr), benzo[*b*]fluoranthene (B[*b*]FA), benzo[*k*]fluoranthene (B[*k*]FA), indeno[1,2,3-*cd*]-pyrene (IdP), dibenz[*a,h*]anthracene (DB[*a,h*]A), and dibenzo-[*a,l*]pyrene were listed as probable or possible carcinogens in humans (*5*, *6*). IARC has recently changed the evaluation of several PAHs, and B[*a*]P is now classified as carcinogenic to humans (group 1) (*7*).

Oxygenated PAHs (oxy-PAHs) such as polycyclic aromatic quinones and polycyclic aromatic ketones are also present in the atmospheric environment, diesel exhaust, and airborne particles as abundant as nonoxy-PAHs (*1*−*4*); however, the toxicological significance of these compounds is not well-studied (*8*, *10*, *11*).

PAHs are considered to induce many kinds of genes such as those coding for metabolic enzymes, P450s, and phase II detoxification enzymes. The pathways for enzyme induction are especially well-known for B[*a*]P (*12*). Metabolic enzymes such as P450s are induced via the aryl hydrocarbon receptor (AhR) by B[*a*]P. AhR is present in cytoplasm as a complex with dimeric heat-shock protein 90 prior to ligand interaction. Ligands such as 2,3,7,8-tetrachlorodibenzo-*p*-dioxin (TCDD) and B[*a*]P activate AhR, and AhR transfers into the nucleus and interacts with the AhR nuclear translocator (ARNT) to form a heterodimeric transcription factor called the AhR complex, which binds xenobiotic response elements (XREs) and mediates the regulation of gene expression including specific P450s, glutathione-S-transferases (GSTs), NAD(P)H-dependent quinone oxidoreductase 1 (NQO1), growth factors, and cytokines.

B[*a*]P is metabolized to many oxygenated derivatives by P450s (*9*). Several electrophilic metabolites of B[*a*]P or reactive oxygen species (ROS) derived from them activate proteins such as activator protein 1 (AP-1) and/or the Nrf2/maf families. These activated proteins bind antioxidant response elements (AREs) or electrophilic response elements (EpREs) and enhance phase II detoxification enzymes such as aldo-keto reductases (AKRs), GSTs, NQO1, and γ-glutamylcystein synthetase (*12*−*17*).

The metabolism of B[*a*]P causes DNA damage, and three major mechanisms have been shown for the activation of DNA adduct formation by B[*a*]P. (i) A radical cation is formed

* To whom correspondence should be addressed. Tel: +81-75-753-5171. Fax: +81-75-753-3335. E-mail: matsuda@eden.env.kyoto-u.ac.jp.
† Department of Environmental Engineering.
‡ Graduate School of Global Environmental Studies.

[1] Abbreviations: PAH, polycyclic aromatic hydrocarbon; IARC, International Agency for Research on Cancer; B[*a*]P, benzo[*a*]pyrene; B[*a*]A, benz[*a*]anthracene; Chr, chrysene; B[*b*]FA, benzo[*b*]fluoranthene; B[*k*]FA, benzo[*k*]fluoranthene; IdP, indeno[1,2,3-*cd*]pyrene; DB[*a,h*]A, dibenz[*a,h*]-anthracene; oxy-PAH, oxygenated PAH; AhR, aryl hydrocarbon receptor; TCDD, 2,3,7,8-tetrachlorodibenzo-*p*-dioxin; ARNT, aryl hydrocarbon receptor nuclear translocator; XRE, xenobiotic response element; GST, glutathione-S-transferase; NQO1, NAD(P)H-dependent quinone oxidoreductase 1; ROS, reactive oxygen species; AP-1, activator protein 1; ARE, antioxidant response element; EpRE, electrophilic response element; AKR, aldo-keto reductase; B[*a*]P-7,8-diol, (±)-*trans*-7,8-dihydroxy-7,8-dihydrobenzo[*a*]-pyrene; BPDE, (±)-*trans*-7,8-dihydroxy-9,10-epoxy-7,8,9,10-tetrahydroben-zo[*a*]pyrene; BPQ, benzo[*a*]pyrene-7,8-quinone; β-NF, β-naphthoflavone; TPh, triphenylene; B[*b*]F, benzo[*b*]fluorene; 3-MC, 3-methylcholanthrene; B[*ghi*]Pe, benzo[*ghi*]perylene; N[*a*]P, naphtho[2,3-*a*]pyrene; BAQ, 7,12-benz[*a*]anthracenequinone; DB[*a,c*]A, dibenz[*a,c*]anthracene; NCQ, 5,12-naphthacenequinone; B[*a*]FO, 11*H*-benzo[*a*]fluoren-11-one; B[*b*]FO, 11*H*-benzo[*b*]fluoren-11-one; B[*c*]FO, 7*H*-benzo[*c*]fluoren-7-one; CPPO, cyclo-penta[*cd*]pyren-3(4*H*)-one; BPO, 6*H*-benzo[*cd*]pyren-6-one; GAPDH, glyce-raldehyde-3-phosphate dehydrogenase; IEF, induction equivalency factor.

10.1021/tx060197u CCC: $37.00
Published on Web 01/25/2007

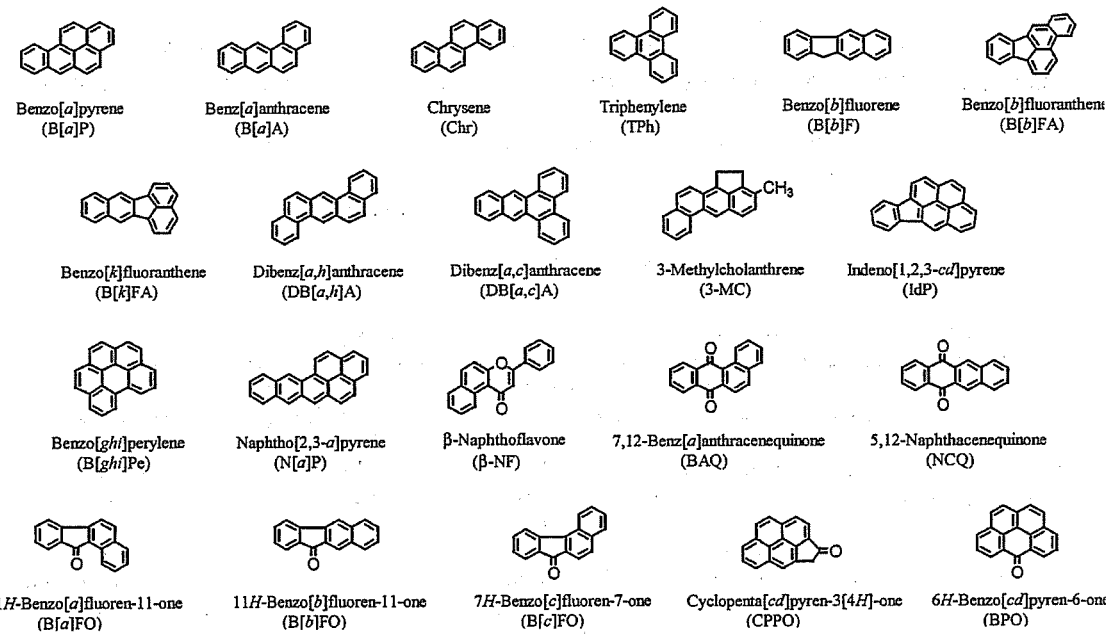

Figure 1. PAHs, oxy-PAHs, and β-NF that were examined in this study.

through a one-electron oxidation, probably via some P450s or peroxidases. This radical cation is considered to form depurinating bulky DNA adducts (*18*, *19*). (ii) B[*a*]P is metabolized to *trans*-dihydrodiols by P450s such as P4501A1 and P4501B1. One, (±)-*trans*-7,8-dihydroxy-7,8-dihydrobenzo[*a*]pyrene (B[*a*]P-7,8-diol), is then changed into a bay region diol epoxide [(±)-*trans*-7,8-dihydroxy-9,10-epoxy-7,8,9,10-tetrahydrobenzo[*a*]-pyrene (BPDE)], which forms stable and depurinating bulky DNA adducts (*9*, *19*). (iii) Suggested by Penning et al. (*12*, *13*, *20*, *21*), B[*a*]P *o*-quinone, benzo[*a*]pyrene-7,8-quinone (BPQ) is formed via AKRs. Four human AKR isoforms (AKR1C1−AKR1C4) catalyze the oxidation of B[*a*]P-7,8-diol to form a B[*a*]P catechol derivative, 7,8-dihydroxybenzo[*a*]pyrene. 7,8-Dihydroxybenzo[*a*]pyrene is then oxidized to BPQ. BPQ enters redox cycles, which are responsible for amplification of free radicals such as semiquinone anion radicals and ROS. This ROS formation is possibly related to both the initiation and the promotion stages of B[*a*]P-induced carcinogenesis (*12*, *22*−*26*).

The reports about metabolic enzyme induction of PAHs except for B[*a*]P are few (*9*, *12*, *13*, *20*, *21*, *27*−*30*). Therefore, in this study, either or both XRE (AhR) and EpRE (AP-1)-mediated typical metabolic enzyme mRNA induction levels (P450s, AKR1C1, GSTM1, and NQO1) in human hepatoma (HepG2) cells caused by 13 representative PAHs and seven oxy-PAHs were examined (Figure 1). These are representative enzymes related to the emergence of DNA adducts and detoxification.

Materials and Methods

Chemicals. TCDD was supplied by Cambridge Isotope Laboratories Inc. (Andover, MA). B[*a*]P, B[*a*]A, Chr, and β-naphthoflavone (β-NF) were supplied by Wako Chemical (Osaka, Japan). Triphenylene (TPh) and benzo[*b*]fluorene (B[*b*]F) were supplied by Tokyo Kasei Co. (Tokyo, Japan). IdP was supplied by Promochem (Wesel, Germany). The other test chemicals were supplied by Sigma-Aldrich Co. (St. Louis, MO). The purity of many test chemicals was 99−100%. The purities of B[*b*]FA, B[*k*]FA, 3-methylcholanthrene (3-MC), benzo[*ghi*]perylene (B[*ghi*]Pe), naphtho[2,3-*a*]pyrene (N[*a*]P), 7,12-benz[*a*]anthracenequinone (BAQ), and β-NF were 98%. The purities of TPh, DB[*a*,*h*]A, dibenz[*a*,*c*]-anthracene (DB[*a*,*c*]A), and 5,12-naphthacenequinone (NCQ) were 97%. The purity of B[*b*]F was 95%.

11*H*-Benzo[*a*]fluoren-11-one (B[*a*]FO), 11*H*-benzo[*b*]fluoren-11-one (B[*b*]FO), 7*H*-benzo[*c*]fluoren-7-one (B[*c*]FO), cyclopenta-[*cd*]pyren-3(4*H*)-one (CPPO), and 6*H*-benzo[*cd*]pyren-6-one (BPO) were synthesized as previously described (*31*−*34*). These compounds were purified by column chromatography and recrystallization. Only the purity of B[*c*]FO was 98%, and the purities of the other four compounds synthesized were greater than 99%.

Qiagen's RNA extraction reagent was purchased from Qiagen (Valencia, CA). Random nonamer, avian myeloblastosis virus-reverse transcriptase, and Ex Taq DNA polymerase were purchased from Takara Bio, Inc. (Otsu, Japan). Me_2SO and methanol, HPLC grade, were purchased from Wako Chemical.

HepG2 Cell Culture and RNA Isolation. The human hepatoma cell line HepG2 was obtained from the Cell Resource Center for Biomedical Research, Institute of Development, Aging and Cancer, Tohoku University, Japan. The cells were maintained in Dulbecco's modified Eagle's medium with 10% v/v fetal bovine serum (*35*). Cells were incubated at 37 °C in a humidified atmosphere containing 5% CO_2. Cells plated on 6 cm dishes were treated for 24 h with test chemicals. All chemicals were dissolved in Me_2SO, and the final concentration of the solvent in the culture medium was 0.1% v/v. Control cells were treated with 0.1% v/v Me_2SO. Total RNA was isolated from the cells using RNeasy Mini Kit (Qiagen) according to the protocol supplied by the manufacture. The RNA was dissolved in RNase free water, and the RNA concentration was determined spectrometrically. Cell cultures were conducted in triplicate for each chemical with each concentration. It was observed that HepG2 cells adhered to the dish were about half the levels in the controls when exposed to 5 μM 3-MC for 24 h. However, such extreme decreases in cell adherence were not observed until 72 h in the case of HepG2 cells that were exposed to other test chemicals.

RT and Real-Time PCR. Total RNA (100 ng) was added to a reaction mixture containing 150 ng of random nonamer, 3.5 units of AMV-RT, 25 mM Tris-HCl buffer (pH 8.3), 50 mM KCl, 2 mM $MgCl_2$, 5 mM dithiothreitol, and 1 mM deoxyribonucleoside triphosphates in a final volume of 21 μL (*35*). The reaction mixture was incubated at 37 °C for 10 min, heated at 55 °C for 30 min, and heated at 99 °C for 5 min to inactivate the enzyme.

Oligonucleotides used for PCR for four genes were commercially synthesized from Sigma Genosys Co. (Ishikari, Japan) as follows:

(i) P4501B1: 5′-TCCTGGACAAGTTCTTGAGG-3′ (508 bp) and 5′-TCAAAGTTCTCCGGGTTAGG-3′. (ii) AKR1C1: 5′-CAGGATTGGCCAAGTCCATC-3′ (256 bp) and 5′-CAAAGGACTGGGTCCTCCAA-3′. (iii) NQO1: 5′-CTGATCGTACTGGCTCACTC-3′ (202 bp) and 5′-GAACAGACTCGGCAGGATAC-3′. (iv) GSTM1: 5′-TCACAAGATCACCCAGAGCA-3′ (364 bp) and 5′-AAAGCGGGAGATGAAGTCCT-3′.

P4501A1 (433 bp), 1A2 (309 bp), and glyceraldehyde-3-phosphate dehydrogenase (GAPDH) (546 bp) primers were used from Takara's Human Cytochrome P450 Competitive RT-PCR Set. Quantification of cDNA was performed using a Smart Cycler System (Cepheid, United States), and staining was carried out with SYBR Green I. A 2 μL portion of the reverse transcriptase mixture was added to a PCR mixture containing 0.2 μM of each primer, 0.3 mM dNTPs, and 0.05 U Ex Taq DNA polymerase in a final volume of 25 μL according to Takara Ex Taq R-PCR Version 2.1 for P4501B1 gene and Version 1.0 for other genes with slight modifications. The PCR reactions were performed with Ex Taq polymerase under the following conditions (95 °C for 3 s and 65 °C for 30 s for the GAPDH and P4501A1, 1A2, and 1B1 genes; 95 °C for 3 s and 66 °C for 30 s for the AKR1C1 gene; 95 °C for 3 s and 60 °C for 30 s for the NQO1 gene; and 95 °C for 3 s and 64 °C for 30 s for the GSTM1 gene). PCR amplifications were carried out for 35 cycles for the GAPDH, P4501A1, AKR1C1, NQO1, and GSTM1 genes, for 40 cycles for the P4501A2 gene, and for 45 cycles for the P4501B1 gene. Specificity of the PCR product was determined by melting curve analysis. The expression was then normalized against the expression of GAPDH.

The concentrations producing P4501A1 mRNA equal to 25% of the maximal amount to TCDD were calculated and expressed as EC_{TCDD25}. The ratios of the EC_{TCDD25} of B[*a*]P to the EC_{TCDD25} of each of the tested compounds were calculated and were referred to as induction equivalency factors (IEFs).

Results

Induction of mRNA of Metabolic Enzymes Measured after Exposure of 5 μM PAHs and Oxy-PAHs for 24 h. The amount of P450s (P4501A1, 1A2, and 1B1), AKR1C1, NQO1, and GSTM1 mRNA in HepG2 cells induced by 5 μM of 20 representative PAHs and oxy-PAHs for 24 h was examined (Figures 2 and 3). The ratio of P4501A1 mRNA levels to GAPDH mRNA of Me_2SO control level was 1.1×10^{-2}. P4501A1 mRNA was induced by 5 μM in the case of most PAHs and some oxy-PAHs. B[*a*]P was 40-fold higher than the Me_2SO control (Figure 2A). The five-ring PAHs such as B[*k*]FA, DB[*a,h*]A, and 3-MC and the six-ring IdP were as high as or higher than the levels of induction by B[*a*]P (38- to ~58-fold). The six-ring PAH N[*a*]P induced at the highest level (80-fold) among compounds examined in this study and the four-ring PAHs B[*a*]A and Chr were slightly lower than the levels of induction by B[*a*]P (both were 29-fold). The levels of induction by four-ring oxy-PAHs, NCQ, BAQ, and B[*b*]FO and four-ring PAH and B[*b*]F were also high (21-, 17-, 15-, and 14-fold, respectively), but polycyclic aromatic ketones such as B[*a*]FO and B[*c*]FO showed low induction levels and six-ring PAH, B[*ghi*]Pe, and a representative AhR ligand, β-NF, which was used for comparison—β-NF is not an atmospheric pollutant—also showed low activities (3-, 2-, 3-, and 3-fold, respectively). The four-ring PAH, TPh, and five-ring PAK, CPPO, induced P4501A1 mRNA at the same levels as the Me_2SO control. The P4501A1 mRNA induction activity by five-ring PAK, BPO, was under half that of the control values (0.4-fold). The ratio of P4501A2 mRNA levels to GAPDH mRNA of Me_2SO control level was 8.5×10^{-4}. The tendency was observed that P4501A2 mRNA induction for test chemicals was similar to that of P4501A1 (Figure 2B). The levels of induction by B[*a*]P, B[*a*]A, Chr, B[*b*]FA, B[*k*]FA, DB[*a,h*]A, IdP, N[*a*]P, BAQ, NCQ, and

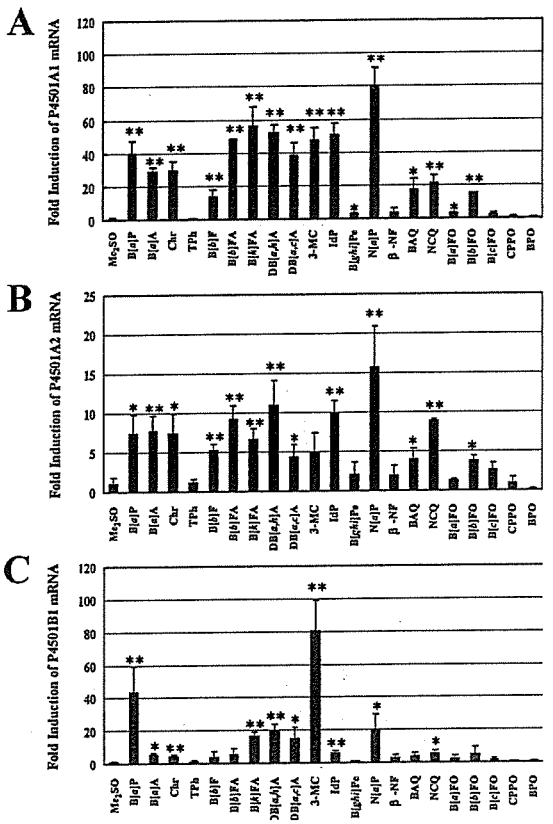

Figure 2. Induction of P450s mRNA measured by RT-PCR in HepG2 cells exposed to 5 μM PAHs and oxy-PAHs for 24 h. (A) P4501A1 mRNA, (B) P4501A2 mRNA, and (C) P4501B1 mRNA were measured. Two asterisks (**) indicate a highly significant difference from control ($p < 0.01$), and one asterisk (*) indicates a significant difference from control ($p < 0.05$) as determined by a *t*-test.

B[*b*]FO were 7-, 8-, 7-, 9-, 7-, 11-, 10-, 16-, 4-, 9-, and 4-fold, respectively. B[*c*]FO, B[*ghi*]Pe, and β-NF showed low activities (3-, 2-, and 2-fold, respectively). TPh, B[*a*]FO, and CPPO induced P4501A2 mRNA at the same levels as the Me_2SO control. The ratio of P4501B1 mRNA levels to GAPDH mRNA of Me_2SO control level was 3.5×10^{-6}. In P4501B1 mRNA induction, 3-MC was very high (80-fold) and B[*a*]P was 44-fold followed by N[*a*]P, DB[*a,h*]A, B[*k*]FA, and DB[*a,c*]A (20-, 20-, 16-, and 15-fold, respectively) (Figure 2C). B[*a*]A, Chr, B[*b*]F, B[*b*]FA, IdP, BAQ, NCQ, and B[*b*]FO were 5-, 4-, 4-, 5-, 6-, 4-, 5-, and 5-fold, respectively. The tendency was also observed that both P4501A2 and P4501B1 mRNA induced by BPO were under half that of the control values (0.1- and 0.5-fold, respectively) similar to P4501A1. The mRNA induction levels for each P450 (P4501A1, 1A2, and 1B1) by most AhR active nonoxy-PAHs were higher than AhR active oxy-PAHs at 5 μM. It was first found that 5 μM nonoxy-PAHs such as B[*b*]F, DB[*a,c*]A, and N[*a*]P and oxy-PAHs such as BAQ, NCQ, and B[*b*]FO induced CYPs.

The ratio of AKR1C1 mRNA levels to GAPDH mRNA of Me_2SO control level was 3.3×10^{-2}. AKR1C1 mRNA levels were very high in one oxy-PAH, B[*a*]FO (11-fold to Me_2SO control), and the levels are close to a representative AhR ligand and AP-1 active compound, β-NF (13-fold to Me_2SO control) (Figure 3A). B[*a*]P, B[*k*]FA, DB[*a,h*]A, NCQ, B[b]FO, and CPPO also induced AKR1C1 mRNA significantly (7-, 7-, 5-, 6-, 5-, and 5-fold, respectively).

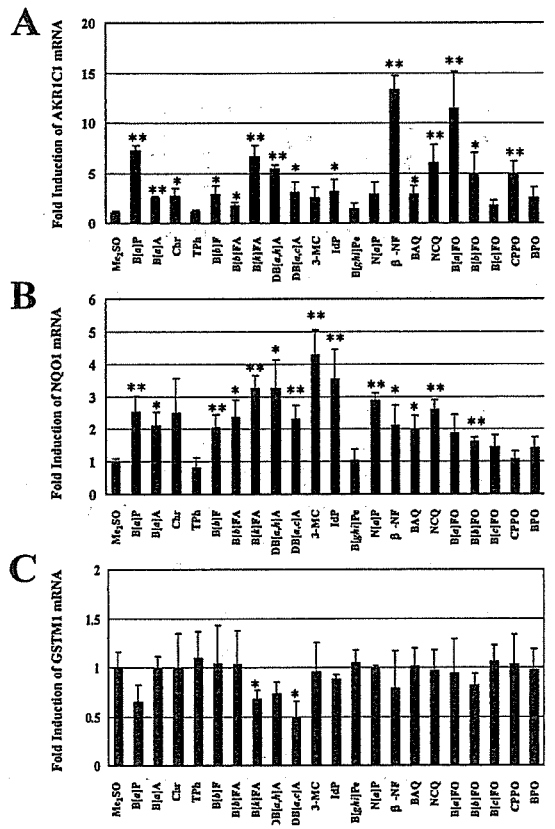

Figure 3. Induction for mRNA of metabolic enzymes measured by RT-PCR in HepG2 cells exposed to 5 μM PAHs and oxy-PAHs for 24 h. (A) AKR1C1 mRNA, (B) NQO1 mRNA, and (C) GSTM1 mRNA were measured. Two asterisks (**) indicate a highly significant difference from control ($p < 0.01$), and one asterisk (*) indicates a significant difference from control ($p < 0.05$) as determined by a *t*-test.

The ratio of NQO1 mRNA levels to GAPDH mRNA of Me_2SO control level was 2.4×10^{-1}. NQO1 mRNA levels were high for 3-MC and IdP (both were 4-fold to control), and B[*a*]P, Chr, B[*k*]FA, DB[*a,h*]A, N[*a*]P, and NCQ all were 3-fold (Figure 3B). The ratio of GSTM1 mRNA levels to GAPDH mRNA of Me_2SO control level was 8.4×10^{-2}. No test chemical induced GSTM1 mRNA significantly. However, GSTM1 mRNA levels of B[*a*]P, B[*k*]FA, DB[*a,h*]A, and DB-[*a,c*]A were lower than the control level (0.6-, 0.7-, 0.7-, and 0.5-fold, respectively) (Figure 3C).

Dose-Dependent Induction of mRNA of Metabolic Enzymes after Exposure to PAHs and Oxy-PAHs for 24 h. The concentration-dependent induction of P450s, NQO1, and GSTM1 mRNA exposed for 24 h to B[*a*]P, B[*k*]FA, DB[*a,h*]A, IdP, NCQ, and B[*b*]FO was also examined (Figure 4). The EC_{25} for the TCDD-dependent induction of P4501A1 mRNA in HepG2 cells was 68 pM (Figure 4A and Table 1). B[*a*]P was approximately 2000-fold less potent than TCDD. Also, in this experiment, PAHs such as B[*k*]FA and DB[*a,h*]A induced P4501A1 mRNA transcription much more strongly than B[*a*]P (100- and 6.7-fold IEF, respectively). Oxy-PAHs, NCQ, and B[*b*]FO induced P4501A1 mRNA transcription less strongly than B[*a*]P; nevertheless, these activities are considered to be high (0.66- and 0.58-fold IEF, respectively). Dose–response curves of P4501A2 mRNA inductions for the six compunds were quite similar to P4501A1, respectively (Figure 4B).

The order of the strength for NQO1 mRNA induction judged from the dose–response curves was as follows, B[*k*]FA, DB-[*a,h*]A, IdP > B[*a*]P, NCQ > B[*b*]FO, and slight NQO1 mRNA induction by 1.6 nM TCDD seemed to be observed (Figure 4C). GSTM1 mRNA induction was slightly decreased by concentration over 500 nM for B[*a*]P and B[*k*]FA and over 5 μM for DB[*a,h*]A and B[*b*]FO (Figure 4D).

Time-Dependent Induction for mRNA of Metabolic Enzymes after Exposure by 5 μM PAHs and Oxy-PAHs. Time–course induction levels of P4501A1, AKR1C1, NQO1, and GSTM1 mRNA by six representative 5 μM PAHs and oxy-PAHs (B[*a*]P, B[*k*]FA, DB[*a,h*]A, IdP, NCQ, and B[*b*]FO) were also examined (Figure 5). The induction of P4501A1 mRNA increased rapidly after exposure for six all PAHs and oxy-PAHs (Figure 5A) and was especially remarkable and continued through 48 h for B[*k*]FA and DB[*a,h*]A. Induction levels were almost constant after 6 h for NCQ and B[*b*]FO.

The mRNA induction of AKR1C1 increased quickly from 6 to 24 h for all PAHs and oxy-PAHs. The increase in rate for mRNA induction of AKR1C1 was higher for oxy-PAHs, NCQ, and B[*b*]FO than for nonoxy-PAHs (Figure 5B). The observed tendency was that the induction of AKR1C1 mRNA for all of the compounds started to decrease after 24 h.

The mRNA induction of NQO1 increased slowly at first but rose quickly from 6 to 24 h for most PAHs and oxy-PAHs. The increase in rate for the mRNA induction of NQO1 was slightly higher for oxy-PAHs, NCQ, and B[*b*]FO than for nonoxy-PAHs (Figure 5C). The induction of NQO1 mRNA started to decrease from about 24 h after for B[*a*]P, NCQ, and B[*b*]FO and was constant from 24 to 72 h for B[*k*]FA, DB-[*a,h*]A, and IdP. The observed tendency for GSTM1 mRNA showed slight decreases in induction for all PAHs and oxy-PAHs until 12 h. This tendency continued until 48 h for B[*a*]P and B[*k*]FA; however, the induction levels started to increase again after 12 h and exceeded control levels for B[*b*]FO, NCQ, IdP, and DB[*a,h*]A (Figure 5D).

Discussion

Some of the main target organs for carcinogenesis by PAHs include lung, skin, and mammary glands; for example, mammal hepatoma cells are often used for examining metabolic enzyme induction and DNA adduct formation by PAHs such as B[*a*]P because the liver induces various metabolic enzymes at relatively high levels. It has also been suggested that liver metabolism plays a role for detoxification of PAHs and oxy-PAHs in local carcinogenesis; therefore, liver cells are appropriate for examining the induction patterns of enzymes related to detoxification.

Several research groups have reported induction of P4501A1 by PAHs in HepG2 cells (*12*, *30*, *35*–*40*), and the order for the strength of the induction was as follows: B[*k*]FA > DB[*a,h*]A > IdP > B[*b*]FA > B[*a*]P > Chr, B[*a*]A. This was determined from data utilizing the luciferase assay after 16 h and the immunoblot assay after 24 h (*37*, *39*). These patterns were similar to our RT-PCR results after 24 h (Figure 4A). In this study, the levels of induction of P4501A1 mRNA by all 5 μM-dosed PAHs and oxy-PAHs did not decrease even after HepG2 cells were continually exposed for 72 h (Figure 5A). The mRNA half-life of P4501A1 is short (2.4 h), while the half-lives of both P4501A2 and P4501B1 mRNA are more than 24 h (*41*). It was reported that more than 75% of approximately 2 μM B[*a*]P was metabolized for 24 h in HepG2 cells and the tendency of metabolism for B[*k*]FA was similar to B[*a*]P (*37*, *42*). Penning et al. suggested that one of the oxygenated metabolites of B[*a*]P, *o*-quinone (BPQ), also contributed to P4501A1 induction in HepG2 cells exposed to B[*a*]P. Therefore, it is possible that some oxygenated metabolites of B[*k*]FA contrib-